UHASSELT
KNOWLEDGE IN ACTION

Maastricht University

Faculty of Medicine and Life Sciences
School for Life Sciences
Master of Biomedical Sciences

Master's thesis

Using pyridoxamine to limit cardiovascular toxicity during doxorubicin chemotherapy

Manon Marie Jager

Thesis presented in fulfillment of the requirements for the degree of Master of Biomedical Sciences, specialization Molecular Mechanisms in Health and Disease

SUPERVISOR :

Prof. dr. Virginie BITO

MENTOR :

De heer Sibren HAESEN

2021
2022

Transnational University Limburg is a unique collaboration of two universities in two countries: the University of Hasselt and Maastricht University.

UHASSELT
KNOWLEDGE IN ACTION

www.uhasselt.be
Universiteit Hasselt
Campus Hasselt:
Martelarenlaan 42 | 3500 Hasselt
Campus Diepenbeek:
Agoralaan Gebouw D | 3590 Diepenbeek

UHASSELT
KNOWLEDGE IN ACTION

Maastricht University

Faculty of Medicine and Life Sciences
School for Life Sciences
Master of Biomedical Sciences

Master's thesis

Using pyridoxamine to limit cardiovascular toxicity during doxorubicin chemotherapy

Manon Marie Jager

Thesis presented in fulfillment of the requirements for the degree of Master of Biomedical Sciences, specialization Molecular Mechanisms in Health and Disease

SUPERVISOR :
Prof. dr. Virginie BITO

MENTOR :
De heer Sibren HAESEN

Using pyridoxamine to limit cardiovascular toxicity during doxorubicin chemotherapy*

Jager Manon Marie[1], Haesen Sibren[1], Deluyker Dorien[1], Wolfs Esther[1] and Bito Virginie[1]

[1]Cardio and organ systems, Biomedical Research Institute, Universiteit Hasselt, Campus Diepenbeek, Agoralaan Gebouw C - B-3590 Diepenbeek

*Running title: *Can pyridoxamine limit DOX-induced cardiotoxicity?*

To whom correspondence should be addressed: Prof. dr. Virginie Bito, Tel: +32 11 26 92 85; Email: virginie.bito@uhasselt.be

Keywords: Doxorubicin, cardiotoxicity, aortic toxicity, pyridoxamine, advanced glycation end-products.

ABSTRACT

Doxorubicin (DOX) chemotherapy-induced cardiotoxicity remains a setback when treating cancer. A substantial amount of cancer survivors experiences cardiovascular problems, causing mortality among this population. The exact mechanisms that cause cardiotoxicity remain unknown. New insights into how DOX induces cardiotoxicity and aortic damage are necessary to meet the unmet need for cardioprotection for cancer patients. Superoxide dismutase (SOD), known to scavenge superoxide scavenger and thus to reduce oxidative stress, was used to diminish acute DOX toxicity. Pyridoxamine (PM), known for inhibiting advanced glycation end-product and reducing inflammation and oxidative stress, was used to limit chronic DOX toxicity. Cardiomyocytes and aortae were isolated. Aortae and cardiomyocytes were acutely exposed to DOX *ex vivo* for 2 h. Chronic exposure included eight weeks of DOX treatment *in vivo*. Doxorubicin caused significant acute and chronic impairment in unloaded cell shortening compared to control cells. PM could limit the increased time to peak contraction after chronic DOX treatment, but not the fractional cell shortening. Doxorubicin-incubated aortic rings showed acute decreased endothelium-dependent relaxation capacity. This impaired relaxation induced by DOX was partially restored with SOD pre-incubation but not significant. Our data have shown that doxorubicin induces cardiovascular toxicity. These data suggest that the DOX-induced toxicity involves multiple mechanisms. These results can provide insights for further research into therapeutical targets to limit the DOX-induced cardiovascular problems, providing a solid basis for new cardioprotective therapies for cancer patients during chemotherapy.

1 INTRODUCTION

1.1 Doxorubicin as anti-cancer treatment

Doxorubicin (DOX) is used to treat a wide variety of cancers, such as breast cancer and advanced sarcomas (1, 2). However, DOX is not only known to attack cancer, but this anthracycline also causes cardiotoxicity (3). Clinicians have already lowered the cumulative dose of DOX to 400-450 mg/m² in order to prevent cardiotoxicity; however, DOX will not be as efficient as needed anymore (4). In spite of DOX causing cardiotoxicity, this chemotherapy is still an often-used cancer treatment, since other anthracyclines such as epirubicin have shown to be less effective in treating cancer (3, 5).

This chemotherapy intercalates with DNA, inhibits DNA and RNA replication, and inhibits topoisomerase IIα in proliferating cells like cancer cells (6). Topoisomerase IIα is an enzyme involved in DNA replication and repair (7). These toxic effects cause cell death in cancer cells and, hence, are responsible for the anti-cancer properties of DOX (6) (Figure 1).

1.2 Doxorubicin affects cardiac function

Despite the importance of chemotherapy in saving lives, cardiovascular problems that arise during treatment remain a serious problem in the field of oncology. DOX inhibits topoisomerase IIα in cancer cells, but in cardiomyocytes, topoisomerase IIβ is affected by the chemotherapy. This causes considerable toxicity

to the cardiovascular system (8) (Figure 1). It is suggested that DOX increases reactive oxygen species (ROS) levels that cause oxidative stress and cell toxicity (8). Furthermore, it has been proposed that DOX decreases the cKit cardiac progenitor cells that, in normal circumstances, are responsible for compensatory mechanisms during stress and vascular injury (8). DOX could also form complexes with iron that give rise to toxic structures resulting in mitochondrial dysfunction (8). All these mechanisms might contribute to cell dysfunction and consequently cell death in the cardiomyocytes. There is still an incomplete understanding of how chemotherapy exactly affects the cardiovascular system. Some agents (e.g., dexrazoxane) are documented to be cardioprotective. Although, dexrazoxane has been associated with myelosuppression (i.e., reduced bone marrow activity) and cannot be used as a cardioprotective therapy (9). Therefore, cardiovascular toxicity in patients undergoing DOX chemotherapy remains a problem without alternatives. Several studies have already documented cardiotoxicity because of DOX chemotherapy (10, 11). Currently, a substantial amount of cancer patients suffers and eventually dies from cardiovascular problems (12). For example, 15% of breast cancer survivors die from cardiovascular disease (CVD) (12). Bradshaw *et al.* (13) showed that chemotherapy-treated female breast cancer survivors show 1.7 fold more CVD-related mortality compared to women without breast cancer. Untreated breast cancer survivors showed a 1.1-fold increase compared to women without breast cancer (13). Cardiotoxicities caused by anthracyclines are, for example, left ventricular dysfunction and congestive heart failure (14). Furthermore, DOX can cardiomyocyte death (e.g., apoptosis, necrosis). A mechanisms that can underly this is oxidative stress due to an increased ROS formation (e.g., superoxide). Superoxide dismutase (SOD) is an enzyme involved in scavenging superoxide and in this way, in reducing oxidative stress (15).

The prevalence of cardiomyopathies rises significantly when doses of DOX exceed 550 mg/kg (14). When a cumulative dose of 430-600 mg/m² DOX is given, contractile dysfunction of the left ventricle occurs in 50-60% of the patients (16). Mortality can be up to 50% when congestive heart failure develops due to DOX treatment (17). DOX-induced cardiotoxicity has also been demonstrated in children aged between one and 15 years old (18). Lipshultz and colleagues (18) have shown that 75% of pediatric patients experienced abnormalities of left ventricular afterload or contractility. This study showed that the cumulative dose of DOX was a significant predictor of abnormal cardiac function (18). Sixty-five percent of patients receiving a minimum cumulative dose of 228 mg/m² showed an increased afterload or decreased contractility

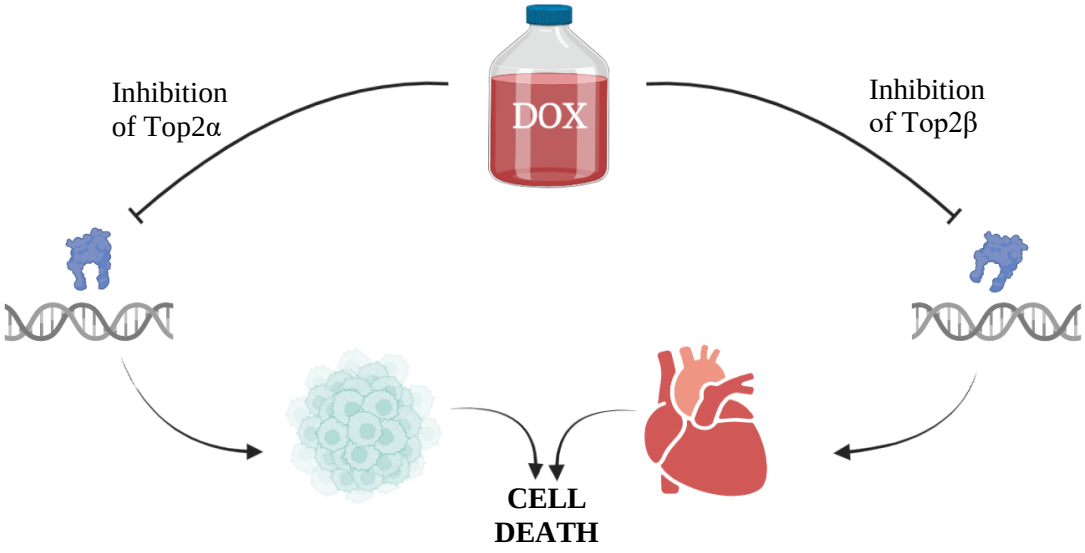

Figure 1. DOX not only attacks cancer cells but also causes cardiotoxicity. DOX inhibits Top2α and Top2β, present in, respectively, cancer cells and cardiomyocytes. DNA damage and consequently apoptosis are desired effects of DOX treatment to attack cancer. However, cardiomyocytes are also damaged by DOX. A proposed mechanism is impairment of mitochondrial function and structure, thereby causing oxidative stress. *DOX, doxorubicin; Top2, topoisomerase 2.*

(18). On the contrary, only 17% of the patients who received only one dose of DOX had an elevated age-adjusted increase in afterload (18).

1.3 Doxorubicin also affects vascular function

DOX not only influences the heart itself, but it affects the complete cardiovascular system. DOX causes significant dysfunction in endothelial cells and vascular smooth muscle cells (VSMCs) in murine models (19, 20). Wojcik *et al.* (21) found that DOX accumulates in endothelial nuclei, induces arterial stiffness, and induces apoptosis. In research performed by Murata *et al.*, DOX-treated rabbit mesenteric arteries showed DNA damage and apoptosis as a result of chronic DOX treatment (22). Furthermore, Bosman *et al.* (23) demonstrated DOX-induced aortic stiffness in mice (23). It was found by Hodjat and colleagues (24) that senescence, hence dysfunction, of VSCMs was induced by DOX incubation *in vitro*.

These negative effects of DOX on aortic stiffness and relaxation have not only been observed in experimental animals but also in human patients. Budinskaya *et al.* (25) demonstrated that arterial wall stiffness was increased in anthracycline-treated patients aged between 16 and 18 years old and between 19 and 24 years old compared to controls. These results suggest that anthracyclines cause toxicity in the arterial wall. Furthermore, Chaosuwannakit *et al.* (26) showed that in participants receiving anthracyclines, aortic stiffness was increased markedly compared to the untreated control group, with effects seen within four months of treatment.

1.4 Link between AGEs and doxorubicin-induced cardiovascular toxicity. Advanced glycation end products (AGEs) are a heterogeneous group of compounds and are widely present in our Western diet. They are formed by the irreversible glycation of proteins (27) and are known to be involved in the development and progression of several diseases, such as cancers and CVD (28). AGEs play a role in CVD development by different mechanisms, including cross-linking of proteins such as collagen, cell signaling (e.g., NF-κβ pathway) by binding to the AGEs receptor (RAGE), and stimulating the formation of ROS causing increased oxidative stress (28-30). Additionally, it is known that AGEs cause endothelial dysfunction (31) and vascular dysfunction by increasing oxidative stress (32). This was also confirmed by our research group (30). In this context, recent studies by our research group investigated the role of AGEs in heart (33) and aorta (30) and showed that AGEs cause significant damage to both heart (e.g., cardiac dysfunction, increased heart mass, cardiomyocyte hypertrophy, remodeling of cardiomyocyte function) and aorta (e.g., dysfunction of contraction and relaxation and wall remodeling). Additionally, our lab showed that pyridoxamine (PM) improved the cardiac phenotype in a rat model for myocardial infarction (34). Hence, PM shows cardioprotective capacities.

1.5 Beneficial effects of pyridoxamine

PM is a natural form of vitamin B_6 known for its capacity to inhibit AGEs, its anti-inflammatory properties, and its antioxidant properties (35). PM forms complexes with metal ions that are responsible for catalyzing oxidative reactions in the protein glycation process (35). Furthermore, PM reacts with carbonyl compounds, which are byproducts of protein glycation, consequently preventing protein damage (35). Additionally, PM possesses anti-inflammatory properties. It does so by, for example, suppressing pro-inflammatory cytokines such as interleukin-1β (36). PM is also known for decreasing oxidative stress. This compound can scavenge ROS via donating a hydrogen atom and, consequently, limit the oxygen and hydrogen radical levels (37). These effects make PM an ideal candidate for an add-on therapy in cancer, since oxidative stress and inflammation are not only important in cardiovascular toxicity but are also key factors in cancer.

Preliminary data from our lab shows that PM can limit DOX-induced heart damage and dysfunction in a non-tumor-bearing animal model. DOX treatment causes cardiotoxicity, characterized by decreased ejection fraction (EF) (Figure 2A) and increased collagen deposition in the myocardium (Figure 2B). Additionally, it was observed that pyridoxamine (PM) was able to limit the DOX-induced cardiotoxicity. As shown by this preliminary data, it has already been determined that the DOX-induced damage to the heart can be limited by PM, indicating a possible role of AGEs, oxidative stress, inflammation, and collagen cross-linking in DOX-induced cardiotoxicity. This data demonstrates the cardioprotective effects of PM. The toxic effects of DOX on cardiomyocytes and aortae damage remain unknown. Additionally, whether PM or

SOD can limit these effects are yet to be discovered.

1.6 Using pyridoxamine to limit DOX-induced cardiovascular toxicity

This study aims to show the use of PM to limit cardiovascular toxicity during chronic chemotherapy. Additionally, we demonstrate the effects of SOD after acute DOX treatment. We hypothesize that SOD and PM can, separately, limit the DOX-induced cardiovascular toxicity after acute and chronic DOX exposure. Several objectives were formulated. With the first objective, we investigate whether aorta and cardiomyocytes are affected by DOX. A second objective aims to demonstrate that SOD can limit acute DOX-induced aortic toxicity. The third objective investigates whether PM can limit cardiomyocyte and aortic toxicity after chronic DOX treatment. Body and organ weights were monitored to assess additional toxicity of DOX.

2 EXPERIMENTAL PROCEDURE

2.1 Experimental design – **General**. In this study, Female Sprague Dawley rats (Janvier, France, 6w, 160-190 g) were used. An acclimatization period of 1 week was included. All animal experiments were performed according to the EU Directive 2010/63/EU for animal testing and were approved by the local ethical committee (Ethical Commission for Animal Experimentation, UHasselt, Diepenbeek, Belgium, ID *in vitro* 202154, ID *in vivo*: 202139). Rats were group-housed in standard cages with cage enrichment at the conventional animal facility of UHasselt. Rats were maintained under controlled conditions regarding temperature (22 °C) and humidity (40–60%). Water and food (Ssniff, Soest, Germany) were provided ad libitum, and rats were handled daily to reduce stress.

***Ex vivo* study**. Fifteen healthy rats were included. Rats were sacrificed, and aortae and cardiomyocytes were isolated. Aortae were divided into the following groups: control group (CTRL), DOX group, DOX + superoxide dismutase (SOD, 150 kU) group, and CTRL+SOD group. Cardiomyocytes were divided into two groups: CTRL group and DOX (1 µM) group. DOX groups were incubated with DOX for 2 h (Supplementary Figure 1A).

***In vivo* study**. A total of 32 rats were included. Animals were divided into four groups: CTRL group, a DOX group, a DOX group receiving PM (DOX+PM), and a CTRL group receiving PM (CTRL+PM). The CTRL groups received 0.9% saline intravenously (i.v.). The DOX animal model was established by a weekly i.v. injection of 2 mg/kg DOX (2 mg/mL, Jessa Hospital, Belgium) for eight weeks. These animals eventually received a cumulative dose of 16 mg/kg of DOX. PM (1 g/L, Santa Cruz, Belgium) was administered via the drinking water

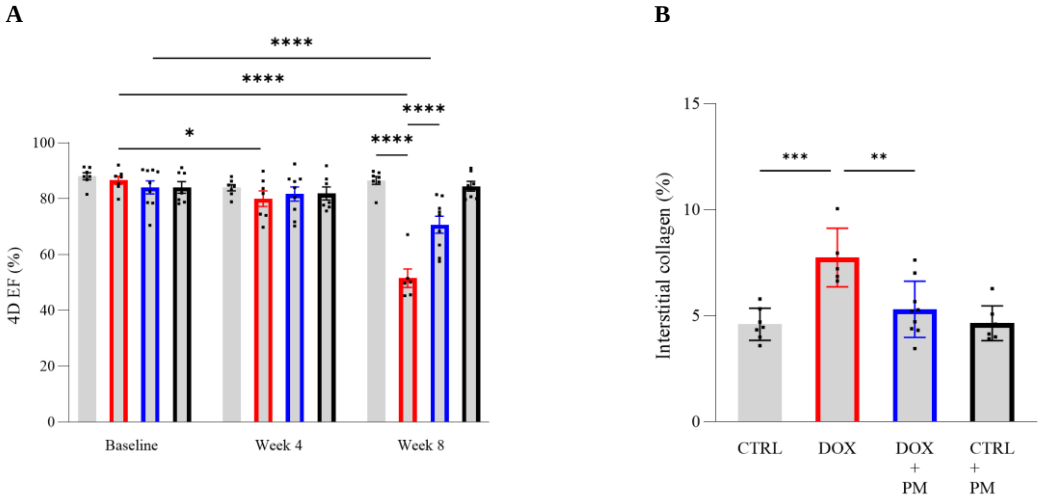

Figure 2. Preliminary data from our lab demonstrating the effect of PM on DOX-induced cardiotoxicity in a rat model. A. 4D ejection fraction. Grey, red, blue, and black bars represent, respectively, CTRL, DOX, DOX+PM, and CTRL+PM groups. **B.** Collagen content in myocardial interstitial space. *PM, pyridoxamine; DOX, doxorubicin; EF, ejection fraction.* *p<0.05, **p<0.01, ***p<0.001, ****p<0.0001

for a total of eight weeks. Body weight was monitored weekly. Cardiomyocytes were isolated after sacrificing (Supplementary Figure 1B).

2.2 Ex vivo unloaded cell shortening measurements – Cardiomyocytes from the left ventricle were obtained by enzymatic dissociation. Isolated cardiomyocytes were placed into a perfusion chamber with normal Tyrode (NaCl 137 mM, KCl 5.4 mM, MgCl2 0.5 mM, CaCl2 1 mM, Na-HEPES 11.8 mM, glucose 10 mM, and taurine 20 mM; pH 7.35) on the stage of an inverted microscope (Nikon Diaphot, Groot-Bijgaarden, Belgium). Unloaded cell shortening of ± eight intact cardiomyocytes per rat was measured with a videoedge detector (Crescent Electronics, London, UK). Field stimulation was done with pulses of constant voltage using platinum electrodes. Steady-state stimuli were applied at frequencies of 1 Hz in the *ex vivo* experiments, and at 1, 2, and 4 Hz in the *in vivo* experiment. Unloaded cell shortening was normalized to diastolic cell length and expressed as fractional cell shortening (L/L_0). Time to peak contraction (TTP) and time to half-maximal relaxation (RT_{50}) were measured to assess kinetics of cell shortening. Reserve contraction was measured after adding isoproterenol (ISO, 300 nM).

2.3 Ex vivo assessment of aortic vasomotor function - **General procedure**. Animals were sacrificed via an overdose of sodium pentobarbital (Dolethal, 150 mg/kg, Val D'hony Verdifarm, Belgium), and heparin (1000 u/kg) was injected. The descending thoracic aorta was isolated and placed in ice-cold Krebs solution (in mM: 118.3 NaCl, 4.7 KCl, 2.5 $CaCl_2$, 1.2 $MgSO_4$, 1.2 KH_2PO_4, 25 $NaHCO_3$, 0.026 EDTA, 5.5 glucose; pH 7.45). The aorta was cleaned of perivascular fat and connective tissue and cut into aortic rings of 3 mm in length. Aortic rings were mounted between two steel hooks, one of which was fixed and the other connected with an isometric force transducer (MLT 050/A, AD Instruments) and a data acquisition system (PowerLab 4/25 T, AD Instruments). Aortic rings were placed in individual tissue baths containing Krebs solution, maintained at 37 °C, and continuously oxygenated. Passive tension (0.8 mV) was applied and rings were equilibrated for 1 h. During this period, aortic rings were washed three times for 20 min with fresh Krebs solution. Aorta experiments were analyzed with LabChart 8 (AD Instruments).

Vasorelaxation response. Precontraction was elicited with 10^{-7} M phenylephrine (PE, Sigma-Aldrich, Diegem, Belgium). After reaching a stable plateau phase, increasing concentrations of acetylcholine (ACh, Sigma-Aldrich) (final bath concentrations of 10^{-10} M to 10^{-5} M) were added to the organ baths to check vessel viability and endothelial integrity (endothelium-dependent relaxation). Dose-response curves were recorded at steady-state after the addition of each concentration of ACh. Aortae that failed to react upon PE or ACh were excluded. The same procedure was repeated with increasing concentrations of sodium nitroprusside (SNP, Sigma-Aldrich) (final bath concentrations of 10^{-10} M to 10^{-6} M) concentrations to assess endothelium-independent relaxation. Relaxation responses were expressed as the percentage of relaxation relative to PE-induced precontraction.

Vasocontraction response. Contractile responses were measured in response to cumulative doses of PE (final bath concentrations: 10^{-10} to 10^{-5} M). Dose-response curves were recorded at steady-state after the addition of each concentration of PE.

2.4 Immunohistochemistry staining (IHC) of *in vivo study* – **General**. For all IHC stainings, transverse sections (7 µm) of paraffin-embedded rat aortic tissue of four different groups (CTRL, DOX, DOX+PM, CTRL+PMPM) were used. Heat-mediated antigen retrieval was performed using citrate buffer (pH 6) for CD68, AGEs, and α-SMA staining or using Tris–EDTA buffer (pH 9) for osteopontin staining. After that, sections were washed with PBS, and 3,3′-diaminobenzidine (DAB) was used for visualization. Endogenous peroxidase was blocked with 30% hydrogen peroxide (H_2O_2) diluted 1:100 in PBS. Afterward, sections were washed with PBS and permeabilized with 0.05% Triton X-100 (Sigma). Then, sections were rewashed, and protein blocking was performed to limit background staining (protein block serum-free, X0909, Dako). Sections were incubated with a primary antibody diluted in PBS for 1 h at room temperature (α-SMA) or overnight at 4 °C (CD68, AGEs, osteopontin), followed by three washes with PBS. Negative controls were incubated with PBS, instead of primary antibody. EnVision™ + Dual Link System-HRP (anti-rabbit/anti-mouse, K4061, Dako) was applied for 30 min at room temperature. The presence of antibody was visualized using 3,3′-diaminobenzidine (DAB). After immunostaining,

nuclei were counterstained using hematoxylin and embedded in DPX mounting medium. Images were acquired using a Leica MC170 camera connected to a Leica DM2000 LED microscope. The level of staining was assessed in eight random fields per section using the color deconvolution plugin in ImageJ software and was expressed as a percentage of the total surface area of interest.

AGEs. Sections were incubated with a primary antibody against AGEs (1:250, ab23722, rabbit anti-rat, Abcam, Belgium). The level of AGEs was obtained via H DAB vector, and total tissue surfaces were obtained via Azan Mallory vector in ImageJ software.

αSMA. Sections were incubated with a primary antibody against α-SMA (1:200, mouse monoclonal, Leica, NCL-SMA). The level of α-SMA was obtained via H DAB vector and total tissue surfaces were obtained via Fuelgen light green.

Osteopontin. Sections were incubated with a primary antibody against osteopontin (1:200, mouse monoclonal Ab ab166709, Abcam). The level of osteopontin was obtained via H DAB vector, and total tissue surfaces were obtained via H&E.

CD68 staining. A primary antibody for CD68 (1/100, mouse monoclonal MCA341R, BIO-Rad) was used to incubate left ventricle (LV) sections. Semi-quantification was done to perform analysis. Score 1: limited number/absence; score 2: minor number; score 3: moderate number; score 4: high number; score 5: high number + presence of aggregates.

2.5 Analysis and statistics – GraphPad Prism 9 was used for the statistical analysis. All variables are continuous, except for the quantification of $CD68^+$ cells (ordinal). Normality was assessed via the Shapiro-Wilk test and visual inspection of the QQ plot. For the analysis of the aorta experiments of the *in vitro* study, cell measurements of the *in vitro* study, and cell measurements of the *in vivo* study, a two-way ANOVA (post-hoc Bonferroni correction) was used in GraphPad Prism. A one-way ANOVA was used to compare AGEs, α-SMA, osteopontin, and CD68 content between rats. When data were not normally distributed, a Kruskal-Wallis (post-hoc Dunn's correction) test was performed. If SDs were not equal, a Brown-Forsythe test (post-hoc Dunnett correction) was performed. Outliers (ROUT method, Q=1%) were excluded from analyses.

3 RESULTS

3.1 DOX causes aortic and cardiomyocyte toxicity *ex vivo*

3.1.1 DOX causes acute impaired cardiomyocyte contractile response *ex vivo*. Six weeks old female rats were sacrificed. After rat cardiomyocytes were isolated, cells were divided into different groups: CTRL group and DOX group. Cell measurements (Figure 3A) at 1 Hz were performed to evaluate the acute effect of DOX on the cardiomyocyte contractility. DOX caused a significant impairment in unloaded cell shortening compared to CTRL cells (Figure 3B) with no difference in kinetics, represented by TTP (Figure 3C) and RT_{50} (Figure 3D). Reserve contraction capacity was not different between groups (Figure 3E).

3.1.2 DOX-induced impaired aortic relaxation is partly attenuated by SOD *ex vivo*. Rat aortae were isolated from six weeks old female rats to assess the acute effect of DOX on aortic function and whether SOD can limit this toxicity. DOX-incubated aortic rings showed decreased endothelium-dependent relaxation capacity after 10^{-3} M and 10^{-2} M acetylcholine compared to CTRL aortic rings (Figure 4A). In line with these results, DOX-incubated aortic rings show a significantly lower E_{max} compared to CTRL rings (Table 1). SNP-induced relaxation was not different between groups (Figure 4B, Table 1).

The effect of SOD on DOX-induced aortic toxicity was assessed. The impaired relaxation induced by DOX was partially restored with SOD pre-incubation but was not significant (Figure 4C). This was also observed in the E_{max} (Table 1) of DOX+SOD which shows a trend toward E_{max} of CTRL rings. SNP-induced relaxation was not different between groups Figure 4D, Table 1).

Tension upon a single dose of PE was compared among the different groups. Tension was higher in DOX-treated aortic rings compared to DOX+SOD rings (Figure 5A). Dose-response of PE was significantly different between DOX and DOX+PM at PE concentrations of 10^{-8} M and 10^{-7} M (Figure 5B).

3.2 DOX causes cardiomyocyte toxicity *in vivo*

3.2.1 PM improves impaired cardiomyocyte contractile kinetics after DOX chemotherapy. Body weight was monitored

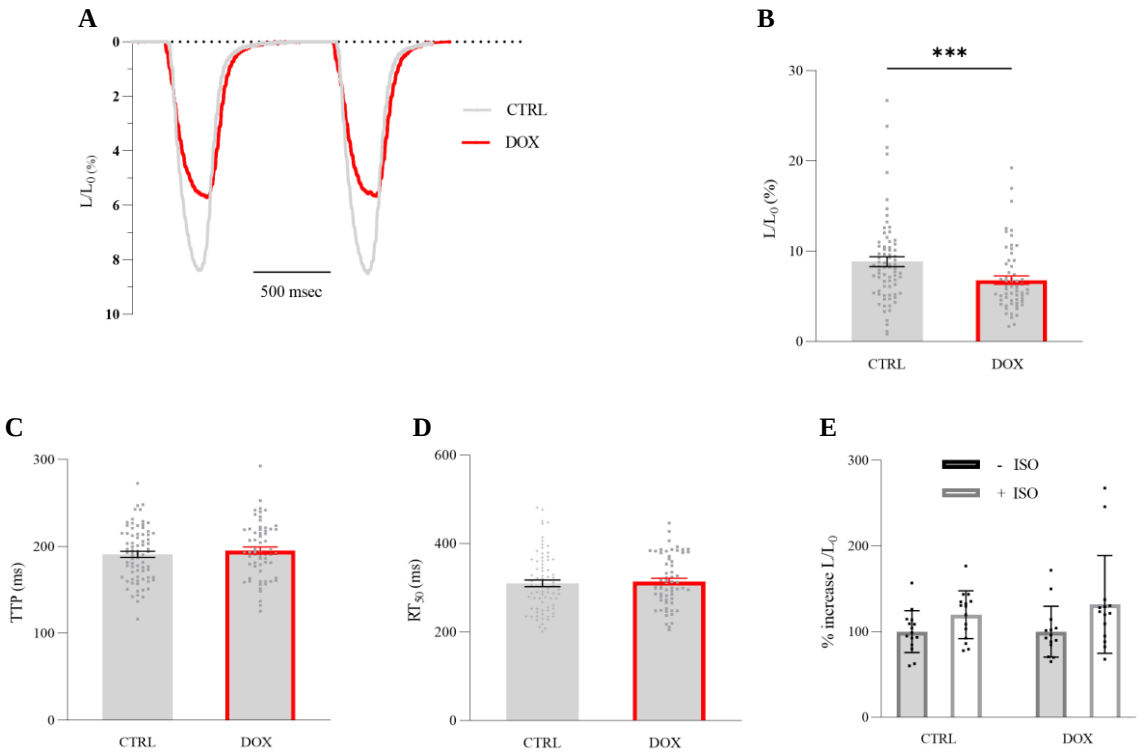

Figure 3. DOX reduces cardiomyocyte contractile properties *ex vivo* at 1 Hz. Cardiomyocytes were collected and incubated in DOX for 2 h (n=76). CTRL cells (n=61) were left untreated. Cell measurements were performed at 1 Hz. **A.** Representation of raw data of cell measurements. **B.** Fractional cell shortening (n_{cells}CTRL=76, n_{cells}DOX=61). **C.** Time to peak contraction (n_{cells}CTRL=77, n_{cells}DOX=62). **D.** Time to half-maximal relaxation (n_{cells}CTRL=77, n_{cells}DOX=62). **For B, C, and D.** $N_{animals}$CTRL=14, $N_{animals}$DOX=9. **E.** Reserve contraction capacity (n_{cells}CTRL=15 (N=5), n_{cells}DOX=14 (N=5)). Data are shown as mean ± SEM. *DOX, doxorubicin; L/L_0, fractional cell shortening; TTP, time to peak contraction; RT50, time to half-maximal relaxation; n, number of cardiomyocytes.* ***p<0.001

weekly (Supplementary Figure 2). CTRL and DOX animals show a significant difference in body weight in week 5, 6 and 7.

After eight weeks of chemotherapy treatment with or without PM of six weeks old rats, cardiomyocytes were isolated. Cell measurements (Figure 6A) at 1, 2, and 4 Hz were performed to demonstrate the cardioprotective effect of PM during DOX chemotherapy treatment. At 2 Hz, fractional cell shortening was significantly lower in DOX group compared to CTRL group (Figure 6B). TTP was significantly different between CTRL and DOX groups, and between DOX and DOX+PM groups (Figure 6C). RT_{50} (Figure 6D) and reserve contraction capacity (Figure 6E) were not different between groups. Additionally, fractional cell shortening was found to be different between DOX and CTRL at 1 Hz (Supplementary Figure 3A) but not at 4 Hz (Supplementary Figure 3B). TTP and RT_{50} were not different at 1 Hz (Supplementary Figure 3C and E) and 4 Hz (Supplementary Figure 3E and F). In addition to this, the number of cardiomyocytes that responded to 2 Hz and 4 Hz stimulation was normalized to 1 Hz stimulation. The percentage of cardiomyocytes that responded to 4 Hz stimulation is lower in DOX group compared to CTRL group and DOX+PM (Supplementary Table 1).

3.2.2 DOX animals show a higher amount of $CD68^+$ cells in the LV tissue. LV sections were stained for CD68. DOX-treated animals show a significantly higher number of CD68+ cells compared to CTRL animals (Figure 7). DOX+PM animals show a trend toward CTRL animals (Figure 7).

3.2.3 AGEs content was not different between groups. Aortae were stained to evaluate AGEs, αSMA, and OPN content in the different groups (CTRL, DOX, DOX+PM, CTRL+PM). With immunohistochemistry, no significant differences in AGEs (Figure 8), αSMA (Supplementary Figure 4A), or OPN (Supplementary Figure 4B) were found between different groups.

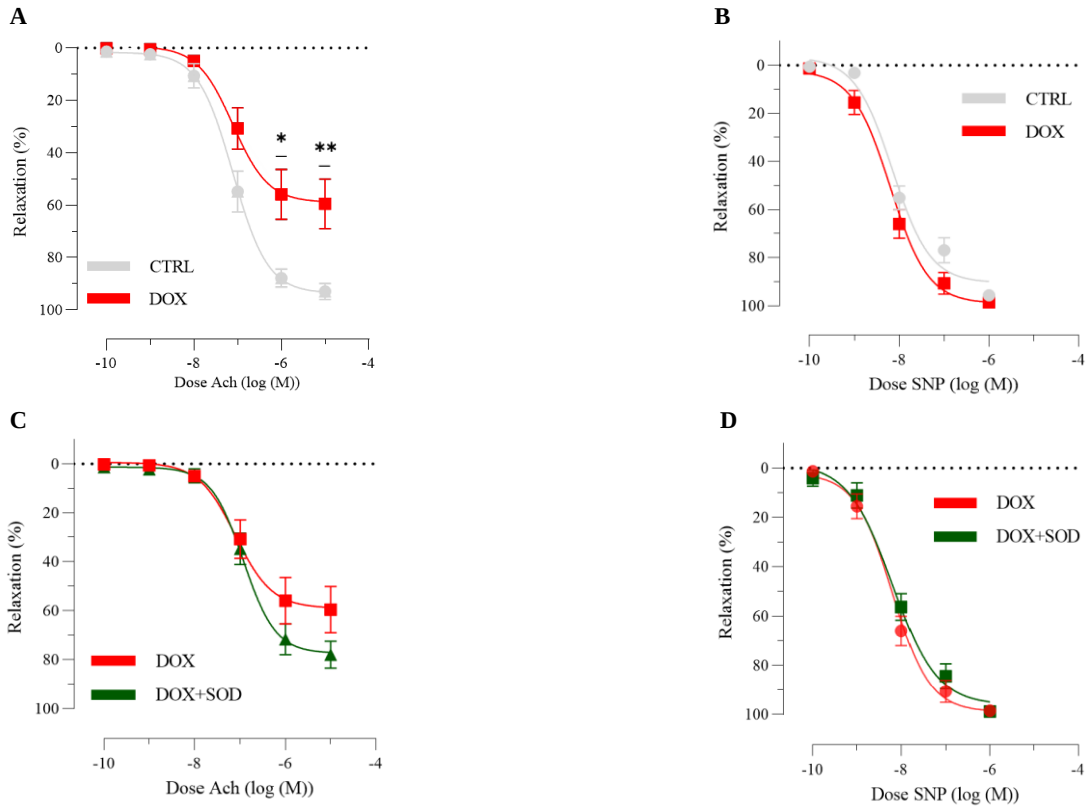

Figure 4. SOD partly restores DOX-induced impairment of endothelium-dependent relaxation. Aortae were isolated from six weeks old female rats. DOX- and DOX+SOD-treated aortic were incubated for 2 h with, respectively, DOX an DOX+SOD. CTRL aortae were left untreated. Vasomotor function was assessed. **A.** Endothelium-dependent relaxation was elicited with ACh (n_{rings}CTRL=15 (N=9), n_{rings}DOX=20 (N=11). **B.** Endothelium-independent relaxation was elicited with SNP (n_{rings}CTRL=21 (N=11), n_{rings}DOX=17 (N=9)). **C.** Endothelium-dependent relaxation was elicited with ACh (n_{rings}DOX=20 (N=9), n_{rings}DOX+SOD=24 (N=11)). **D.** Endothelium-independent relaxation was elicited with SNP (n_{rings}DOX=17 (N=9), n_{rings}DOX+SOD=26 (N=11)). *DOX, doxorubicin; SOD, superoxide dismutase; ACh, acetylcholine; SNP, sodium nitroprusside.* *p<0.05, **p<0.01

Table 1 – E_{max} and logEC_{50} values for ACh- and SNP-induced relaxation after acute DOX treatment and SOD pre-incubation.

	Groups	E_{max} (%)	LogEC_{50} (M)
ACh	CTRL	92.9 ± 3.0	-7,11 ± 0,12
	DOX	59.5 ± 9.3**	-6,77 ± 0,14
	DOX+SOD	77.9 ± 5.4	-6,78 ± 0,12
SNP	CTRL	95,62 ± 1,16	-8,14 ± 0,07
	DOX	98,51 ± 1,05	-8,11 ± 0,10
	DOX+SOD	98,86 ± 0,53	-8,33 ± 0,11

The maximal relaxation response (E_{max}) to ACh and SNP and the required dose for half-maximal response (EC_{50}) were obtained from dose-response curves of ACh and SNP via nonlinear regression. DOX and DOX+SOD aortic rings were incubated for 2 h, respectively, in DOX and in DOX and SOD. CTRL aortic rings were left untreated. Endothelium-dependent relaxation was elicited with ACh (n_{rings}CTRL=15 (N=9), n_{rings}DOX=20 (N=9), n_{rings}DOX+SOD=24 (N=11)). Endothelium-independent relaxation was elicited with SNP (n_{rings}CTRL=21 (N=11), n_{rings}DOX=17 (N=9), n_{rings}DOX+SOD=26 (N=11)). Data are expressed in mean ± SEM. *DOX; doxorubicin; SOD, superoxide dismutase; ACh, acetylcholine; SNP, sodium nitroprusside; n, number of aortic rings.* **p<0,01 DOX vs CTRL

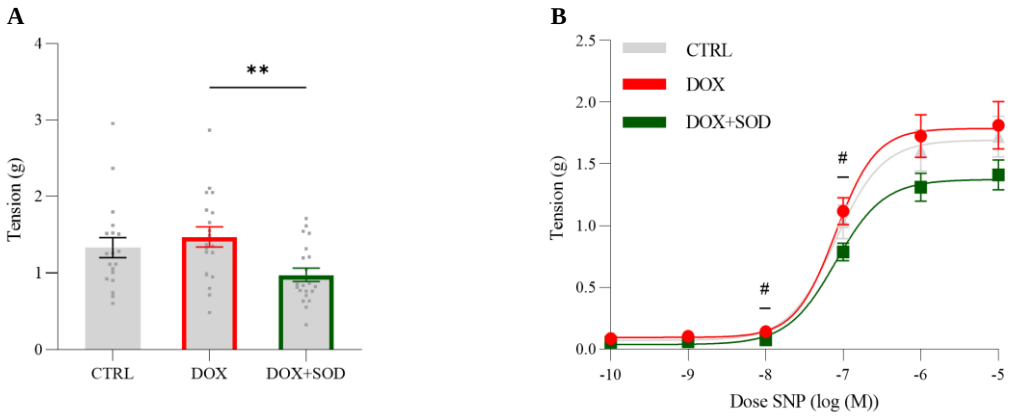

Figure 5. DOX-incubated aortic rings show a higher tension upon a single dose of PE. Aortae were isolated from six weeks old female rats. DOX and DOX+SOD, respectively, were incubated for 2 h with DOX or with DOX and SOD. CTRL rings were left untreated. **A.** Contraction (tension) upon a single dose of PE (final bath concentration: 10^{-7} M) (n_{rings}CTRL=19 (N=9), n_{rings}DOX=19 (N=10), n_{rings}DOX+SOD=21 (N=10)). **B.** Dose-response of PE (final bath concentrations: 10^{-10} to 10^{-5} M) (n_{rings}CTRL=25 (N=13), n_{rings}DOX=22 (N=11), n_{rings}DOX+SOD=26 (N=11)). *DOX, doxorubicin; SOD, superoxide dismutase; PE, phenylepinephrine.* **p<0,01, #p<0.5 DOX vs DOX+SOD

4 DISCUSSION

Currently, DOX-induced cardiovascular toxicity dramatically reduces the patient's quality of life. In this study, we show the detrimental effects of DOX on the cardiovascular system in a rat model and possible mechanisms by which DOX causes toxicity. DOX affects cardiomyocyte contractile response *ex vivo* and *in vivo*. We demonstrate the toxic effects of DOX on endothelium-dependent aorta relaxation *ex vivo*. We show that SOD partly limits this impaired endothelium-dependent aorta relaxation. We show the beneficial effects of PM on DOX-induced cardiovascular toxicity. Research into possible cardioprotection during chemotherapy remains highly important. Even, the second hit hypothesis suggests that exposure to anthracyclines impairs the ability of the heart to adapt to new stress situations (38), highlighting the importance of cardioprotection during chemotherapy.

4.1 Cardiomyocytes show impaired contractile response after acute exposure to DOX. After cardiomyocyte isolation and DOX incubation (2 h, 1 µM), cell measurements were performed at 1 Hz. Fractional cell shortening was significantly lower in DOX-treated cardiomyocytes. Cell kinetics (i.e., TTP and RT_{50}) and reserve contraction capacity were not different, indicating that *in vitro* exposure to DOX only affects contractile response. Xu *et al.* (39) also showed contractile dysfunction of cardiomyocytes after acute exposure to DOX. They incubated the cells for 24 h in DOX (1 µM). In line with our results, Xu *et al.* showed that DOX-incubated cardiomyocytes had a significantly lower fractional cell shortening compared to CTRL cardiomyocytes (39). In contrast, as we have hown, Xu *et al.* (39) showed no difference in TTP. They show no difference in time to 90% relaxation (TR_{90}) (39); in contrast, we show no difference in TR_{50}. This indicates that, even after 24 h of DOX incubation, relaxation is not impaired. In addition to the study of Xu *et al.*, we show the hyper-acute effect of DOX on cardiomyocytes. Our results demonstrate that DOX toxicity is already present after 2 h of DOX incubation. Additionally, relaxation has shown not to be impaired. Contractility impairment might be due to, for example, oxidative stress and disruption of intracellular and mitochondrial Ca^{2+} levels caused by DOX, causing dysfunction in contraction capacity of the cardiomyocytes (40, 41). Oxidative stress is known as the imbalance between detoxifying reactive intermediates and ROS levels. ROS species can cause DNA damage (e.g., DNA-protein cross-links, sugar alterations, strand breaks) (42). Ca^{2+} is crucial for the physiological functioning of cardiomyocytes. Upon the depolarization of the cell membrane, Ca^{2+} is allowed to enter the cell via the L-type Ca2+ channels, consequently inducing Ca^{2+}-induced Ca^{2+}-release out of the sarcoplasmic reticulum. By the binding of Ca^{2+}, troponin-tropomyosin complexes undergo conformational

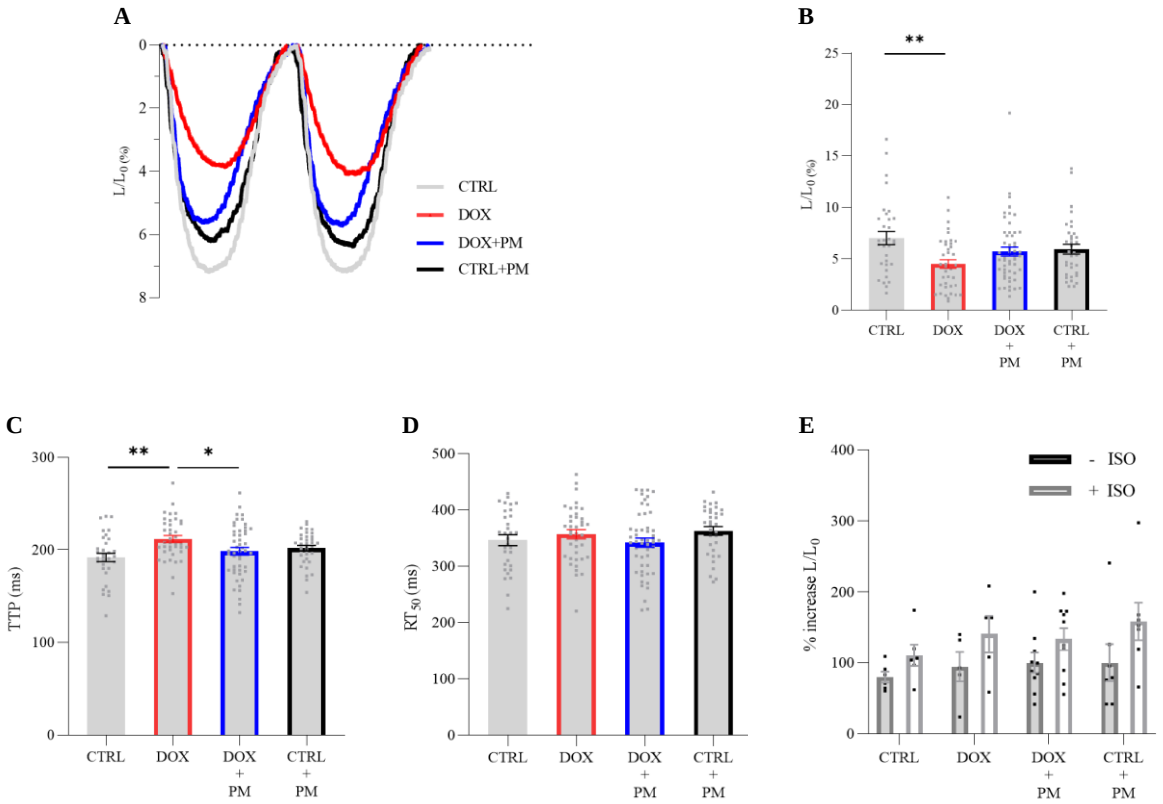

Figure 6. DOX causes significant impairment in contractile properties of cardiomyocytes *in vivo* at 2 Hz. DOX treated animals received weekly i.v. DOX injections (2 mg/kg) for eight weeks. PM treated animals received PM ad libitum via drinking water. CTRL animals were left untreated. Cardiomyocytes were isolated from the heart via enzymatic dissociation and cell measurements were performed at 2 Hz. **A.** Representation of cell measurement data. **B.** Fractional cell shortening (n_{cells}CTRL=32, n_{cells}DOX=39, n_{cells}DOX+PM=52, n_{cells}CTRL+PM=35). **C.** Time to peak contraction (n_{cells}CTRL=32, n_{cells}DOX=39, n_{cells}DOX+PM=49, n_{cells}CTRL+PM=35). **D.** Time to half-maximal relaxation (n_{cells}CTRL=32, n_{cells}DOX=39 n_{cells}DOX+PM=50, n_{cells}CTRL+PM=33). **For B, C, and D.** $N_{animals}$CTRL=5, $N_{animals}$DOX=7, $N_{animals}$DOX+PM=7, $N_{animals}$CTRL+PM=7. **E.** Reserve contraction capacity (% increase L/L_0) after addition of ISO (n_{cells}CTRL=6 (N=3), n_{cells}DOX=5 (N=3), n_{cells}DOX+PM=10 (N=5), n_{cells}CTRL+PM=7 (N=3)). Data are shown as mean ± SEM. *DOX, doxorubicin; PM, pyridoxamine; L/L_0, fractional cell shortening normalized to cell length; TTP, time to peak; RT50, time to half-maximal relaxation; ISO, isoproterenol.* *p<0.05, **p<0.01

changes inducing the excitation-contraction coupling and consequently causing contraction reticulum. By the binding of Ca^{2+}, troponin-tropomyosin complexes undergo conformational changes inducing the excitation-contraction coupling and consequently causing contraction (33, 43). When Ca^{2+} levels are disrupted by DOX, this can have a serious impact on the contractility of cardiomyocytes and eventually on general cardiac function. Impaired contraction of cardiomyocytes will lead to a weakened heart, thus causing DOX-induced cardiotoxicity.

4.2 Aortae show impaired endothelium-dependent relaxation after acute exposure to DOX. *Ex vivo* DOX-incubated aortic rings showed an impaired relaxation response to ACh. ACh elicits an endothelium-dependent relaxation of the aortae's smooth muscle cells. ACh binds its muscarinergic receptor on endothelial cells and consequently causes nitric oxide (NO) production in these cells. This signaling molecule is then converted to cyclic guanosine monophosphate (cGMP), causing a relaxation response in the smooth muscle cell. Relaxation response to SNP was not impaired. SNP causes an endothelium-independent relaxation via directly inducing NO production in the smooth muscle cells. These results indicate that aorta endothelium has been damaged by DOX incubation. This dysfunctional relaxation capacity can cause an increased afterload of the heart and consequently contribute to DOX-induced cardiotoxicity (30). One study by Bosman *et al.* (44) incubated *ex vivo* aortae from mice in DOX (1 µM) for 16 h. They showed an impaired ACh-induced impaired relaxation

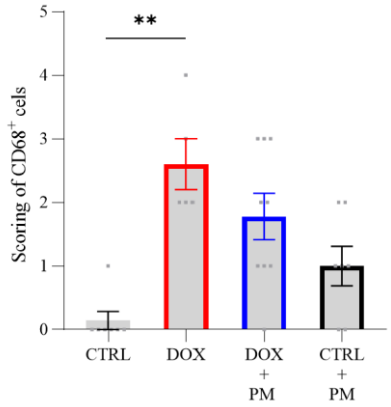

Figure 7. DOX increases the number of CD68⁺ cells in heart tissue. DOX treated animals received weekly i.v. DOX injections (2 mg/kg) for eight weeks. PM treated animals received PM ad libitum via drinking water. CTRL animals were left untreated. Heart sections of CTRL ($N_{animals}$=7), DOX ($N_{animals}$=5), DOX+PM ($N_{animals}$=9), and CTRL+PM ($N_{animals}$=7) were stained with IHC for CD68. Semi-quantification was done to perform analysis. Score 1: limited number/absence; score 2: minor number; score 3: moderate number; score 4: high number; score 5: high number + presence of aggregates. Data are shown by mean ± SEM. *DOX, doxorubicin; PM, pyridoxamine.* **p<0.01

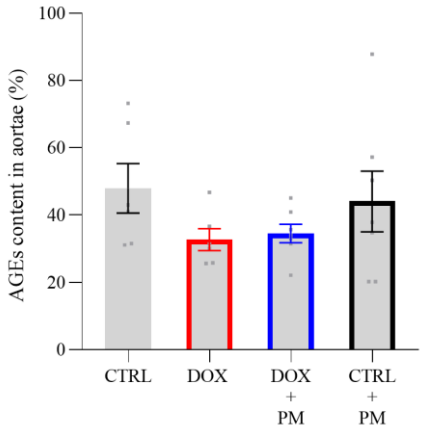

Figure 8. AGEs are not different between groups. Animals were divided into four groups: CTRL, DOX, DOX+PM, and CTRL+PM. After eight weeks of weekly DOX treatment (2 mg/kg), aortae were isolated. Immunohistochemistry was done for AGEs content in aortae ($N_{animals}$CTRL=6; $N_{animals}$DOX=6; $N_{animals}$DOX+PM=7; $N_{animals}$CTRL+PM=7). For every animal, on average eight random fields were used to assess staining. Images were analyzed with ImageJ. Data are shown as mean ± SEM. *AGEs, advanced glycation end-products; DOX, doxorubicin; PM, pyridoxamine; IHC, immunohistochemistry.*

(p<0.05), demonstrating the acute effects of DOX. In addition to this, we show in our study that DOX-incubation (1 µM) already damages aortae relaxation after 2 h. This is in line with what we observed after cardiomyocytes were incubated with DOX. In our research, we demonstrate the hyper-acute DOX-induced toxicity, and Xu *et al.* (39) showed the acute DOX-induced toxicity. These results indicate that DOX toxicity is already reflected in cardiomyocytes and aortae very early. In addition to the previously mentioned findings, we show that the E_{max} after ACh-induced relaxation was significantly reduced after DOX exposure, again indicating the detrimental effects DOX has on aortae endothelium.

4.3 Reducing oxidative stress could partially restore *ex vivo* DOX-induced impaired aortic relaxation. Oxidative stress is characterized by ROS levels (e.g., superoxide) that exceed the antioxidant properties of the cell. SOD is an enzyme responsible for converting superoxide to oxygen and hydrogen peroxide. This enzyme is

extremely important for cellular life, since superoxide causes DNA damage by promoting the production of hydroxyl radicals (45). Consequently, SOD is involved in reducing oxidative stress and preventing superoxide-induced DNA damage. In addition to these antioxidant properties, byproducts of the superoxide conversion act as signaling molecules in various processes (e.g., enzymatic reactions, mitochondrial respiration). Thus, SOD possesses a dual role: reducing oxidative stressing and cell signaling (15). The ability of SOD to reduce oxidative stress is an interesting property, because DOX-induced damage might involve oxidative stress (8). Pre-incubation with SOD was partly able to limit DOX-induced endothelium-dependent impaired relaxation. These data demonstrate that oxidative stress is involved in the DOX-induced impaired relaxation and additionally that oxidative stress is not the only mechanism contributing to DOX-induced aortic toxicity. Kalivendi *et al.* (46) have demonstrated that DOX exposure (0.5 µM) to Bovin Aorta Endothelial Cells (BAECs) for 16 h causes an increase in oxidative stress compared to control cells. In addition to this, Wojcik *et al.* (21) showed that DOX accumulates in EA.hy926 endothelial cells nuclei and suggested that the endothelial stress response due to DOX-induced damage causes the generation of ROS causing oxidative stress (21). Additionally, Kotamraju *et al.* (47) found that DOX (1 µM) causes an increase in superoxide generation in BAECs after 16 h of incubation. These data indicate a major role for oxidative stress in DOX-induced vascular toxicity. Our study demonstrates that SOD can restore impaired aortic relaxation. Hattori *et al.* (48) also demonstrate a beneficial role of SOD for impaired aortic relaxation. They demonstrated that SOD recovers altered endothelium-dependent relaxation in diabetic rat aortae (48). In addition to this, Lund *et al.* (49) showed that gene transfer of SOD improved aortic relaxation after endotoxin incubation. Taken all these results together, SOD has potent beneficial effects on impaired relaxation in aortae. Besides oxidative stress, other mechanisms contributing to DOX-induced toxicity can be impaired NO signaling or production by endothelial NO synthase (eNOS). Bosman *et al.* (23) showed in an *in vivo* study that a weekly DOX injection (4 mg/kg) for two weeks significantly decreased NO levels in mice aortae. These results suggest a major role for NO in DOX-induced impaired relaxation. In our study, the impaired relaxation might also be due to a decrease in NO levels in these DOX-treated animals. Li *et al.* (50) demonstrated that promoting NO production can alleviate DOX-induced endothelium-dependent dysfunction. Based on these results, SOD shows promising aortic protective effects and is worth investigating further. Future experiments can include testing multiple doses of SOD or combining SOD with anti-inflammatory compounds to assess potential synergistic effects.

PE is a compound that elicits contraction in the vascular system. It does so by activating various calcium channels in aorta's smooth muscle cells (51). In our study, no differences between CTRL and DOX aortae were seen in tension after a single dose of PE and in PE dose-response curve. However, Bosman *et al.* (44) demonstrated a lower tension after a single dose of PE ($p<0.0001$) and a difference in PE dose-response curve ($p<0.05$) between CTRL and DOX. These differences can be explained by the higher concentration (2 µM compared to 1 µM) and longer incubation time (16 h compared to 2 h) applied in the study of Bosman *et al.* compared to our study. These data indicate that hyper-acute effects of DOX used in our study (2 h) did not yet impair PE-induced contraction, in contrast to the acute effects of DOX (16 h) shown by Bosman *et al.* This suggests that Ca^{2+} levels, highly important for contraction, are not yet impaired after 2 h of incubation, but are affected by DOX on a later timepoint. In addition to this, we show that SOD significantly lowers ($p<0.01$) tension after a single dose of PE. Even though no difference was seen between DOX and CTRL, we can still suggest a beneficial effect of SOD. The same effect can be observed in the dose-response of PE. These results also demonstrate that SOD significantly lowers tension in aortae at PE concentrations of 10^{-8} M and 10^{-7} M. No significant differences were seen at higher PE concentrations (10^{-6} M and 10^{-5} M); however, this can be explained by the higher variation at these concentrations and because maximal tension is being reached at these concentrations. When taken these results together with the effect of SOD on DOX-induced impaired aortic relaxation, SOD partially improves relaxation and significantly reduces tension.

As previously mentioned, acute DOX exposure causes cardiomyocyte contractile dysfunction. We have shown in this study that reducing oxidative stress by SOD could partially restore the DOX-induced acute aortic relaxation impairment. Since oxidative stress is thought to

be a major player in DOX-induced toxicity (52), SOD might also be beneficial for the DOX-induced cardiomyocyte contractile dysfunction.

4.4 Cardiomyocytes show impaired contractile response after rats were chronically exposed to DOX *in vivo.* Preliminary data from our lab show that eight weeks of chronic DOX (weekly i.v. injection of 2 mg/kg) treatment worsens the 4D EF significantly compared to animals that were left untreated. Consequently, this causes cardiotoxicity. Data from our study confirm these results on a cellular level. Fractional cell shortening and TTP at 2 Hz stimulation were significantly lower in cardiomyocytes isolated from DOX-treated animals compared to cells isolated from CTRL animals. RT_{50} and reserve contraction capacity were not different. At 1 Hz, a difference in fractional cell shortening was observed between CTRL and DOX, and no differences were seen in cell kinetics (TTP and RT_{50}). These data indicate that DOX significantly impairs contractile response in cardiomyocytes and does not impair relaxation. In line with our data at 1 Hz stimulation, Takaseya *et al.* (53) demonstrate an impaired fractional cell shortening of cardiomyocytes after chronic DOX treatment *in vivo*. In this study, male rats received six i.p. DOX injections (2.5 mg/kg) in two weeks (53). In addition, they show a significant difference in TTP and RT_{50} between CTRL and DOX ($p<0.05$). Although the cumulative dose of DOX is comparable (15 mg/kg vs. 16 mg/kg) between Takaseya *et al.* and our study, the time interval between injections in the study of Takaseya *et al.* is shorter compared to our study (two days vs. one week). Demonstrating the timing of DOX dosing is extremely important in the detrimental effects of DOX on cardiomyocytes. The impaired contractile response after DOX treatment can be explained via mechanisms such as oxidative stress or disruption of Ca^{2+} homeostasis (see above). When comparing these results to the *ex vivo* DOX-treated cardiomyocytes in this study, we can conclude that acute and chronic DOX exposure do not impair relaxation response of cardiomyocytes. Additionally, chronic DOX treatment causes a difference in TTP at 2 Hz, in contrast to the acute DOX treatment. This suggests that the time needed for contraction significantly worsens during chronic DOX treatment and that this event is not yet present after acute treatment.

Our preliminary data show that PM improved 4D EF and interstitial collagen of DOX+PM animals compared to DOX animals. Indicating that PM has a cardioprotective effect. We were able to confirm this on a cellular level. PM improved the observed increase in TTP in DOX+PM animals. These results suggest that PM can limit this DOX-induced contractile dysfunction. In contrast, we demonstrate that DOX causes a significant decrease in fractional cell shortening in cardiomyocytes, but without improvement of PM. We expected an improvement due to PM on fractional cell shortening. However, a lot of variation was observed in contrast to 4D EF and interstitial collagen data. This might explain the absence of beneficial cardioprotective effects. Additionally, the mode of administration via drinking water might cause loss of PM and could explain the ineffectiveness of PM on DOX-induced impaired contractile response in cardiomyocytes. This can be explained by a study by Hu *et al.* (54). They injected miRNA-200a, shown to be anti-inflammatory (55, 56) like PM, i.v. via the tail vein of mice and demonstrated a protective effect on the DOX-induced damage (54). Fractional cell shortening was significantly improved after in DOX mice (54). However, DOX treatment started four weeks after the miRNA200a injection (54), suggesting that combining pre-incubation with and an i.v. injection of a cardioprotective compound is shows beneficial effects.

Reserve contraction was elicited by ISO. ISO was used to elicit reserve contraction capacity. This compound, known as isoprenaline and resembles epinephrine structurally, is a $beta_1$ and $beta_2$ adrenergic receptor agonist. Upon binding to the extracellular domain of the receptor, an increase in contraction is caused, which allows us to calculate the reserve contraction capacity. Consequently, causing an increase in contraction of the cardiomyocyte. Reserve contraction capacity was not different between groups. This indicates that, although contractile response was impaired due to chronic DOX treatment, the fractional reserve construction capacity was not different. These data again illustrate that DOX only affects the contractile properties of cardiomyocytes.

The percentage of cardiomyocytes able to contract after stimulation with 4 Hz, the highest field stimulation used in this study, is lower in DOX-treated animals compared to CTRL and DOX+PM animals (Supplementary Table 1). This can possibly be explained by the fact that

DOX damages the cells by causing impaired Ca^{2+} homeostasis and inducing oxidative stress (see above) (41), making contractility at 4 Hz for cardiomyocytes of DOX-treated animals more difficult. These data again demonstrate the detrimental effects of DOX on cardiomyocytes.

4.5 Inflammation plays a role in DOX-induced toxicity. As generally known, inflammation plays a major role in damage and toxicity. We expect inflammation to also play a role in DOX-induced cardiovascular toxicity. Macrophages are known to be involved in inflammation processes and infiltrate damaged tissue (57). Here, we investigated $CD68^+$ cells (general macrophage marker) content in LV tissue. Zhang *et al.* (58) found that $CD68^+$ macrophages were increased in heart tissue from patients that experienced DOX-induced cardiomyopathy, demonstrating the infiltration of these inflammatory cells into heart tissue during DOX chemotherapy. Toll-like receptor 4 (TLR4), a key regulator of inflammation and expressed by macrophages, is known to be involved in cardiac pathogenesis (e.g., cardiac inflammation, oxidative stress (59)) (60, 61) and has an increased expression during DOX-induced cardiomyopathy (62). As shown by Wang *et al.* (63), Toll-like receptor 4 (TLR4) is upregulated in macrophages after DOX incubation for 24 h compared to CTRL cells ($p<0.05$). In heart tissue, other immune cells have also been shown to be increased after DOX treatment. For example, $CD4^+$ lymphocyte levels (i.e., T helper cells) and dendritic cells were increased after 3, 6, 9, and 12 weeks of weekly DOX injections (1 mg/kg) ($p<0.05$) (Zhang *et al.*) (64). Dendritic cells are known to trigger inflammation (65), indicating that an increase in dendritic cells can contribute to DOX-induced inflammation. Although CD4 is a general T lymphocyte marker and thus, no specific subsets can be defined, we can conclude that there is a significant increase in T lymphocyte infiltration into heart tissue. Our results demonstrate a significant increase in macrophages in heart tissue in DOX-treated animals compared to CTRL animals. Zhang *et al.* also show an increase in macrophages after 3, 6, 9, and 12 weeks of weekly DOX injections (1 mg/kg) ($p<0.05$) (64). Taken all these results together, it can be suggested that there is a significant increase in immune cell infiltration into heart tissue due to DOX chemotherapy and that this event contributes to DOX-induced cardiotoxicity. These data provide a solid base to further investigate DOX-induced cardiac inflammation. Additionally, we show an improving trend of $CD68^+$ cells in heart tissue when DOX animals were treated with PM. No significant difference was found, but this could be explained by the high variation seen (e.g., due to the rather low sample size).

4.6 Advanced glycation end-products are no key factor in DOX-induced vascular toxicity. AGEs have been shown to be involved in cardiovascular problems (28). Based on this knowledge, PM, known as an AGEs inhibitor, could limit AGEs formation in aortae and consequently limit DOX-induced aortic problems. However, the percentage of AGEs content in aortic tissue did not differ between groups. Moriyama *et al.* (66) showed that, after eight weeks of weekly i.v. DOX (2 mg/kg) injections of male rats, pentosidine ($p<0.05$) and Nε-(carboxymethyl)lysine ($p<0.05$), two AGEs, were significantly increased in heart tissue of DOX-treated animals compared to CTRL animals. This increase was partially restored by i.p. given PM in DOX-treated animals. These data demonstrate that these AGEs are increased in heart tissue after DOX treatment and suggest an important role for AGEs in DOX-induced cadiotoxicity. In our study, we investigated the AGEs levels in aorta. Our data suggest that AGEs do not play a role in DOX-induced aortic damage.

αSMA and OPN were not different between groups. αSMA is highly important for vascular mechanical tension (67). Also, αSMA has been shown to contribute to motility and contraction of smooth muscle cells present in aorta (68, 69). Here, our data show that DOX did not affect αSMA content in aortae and consequently suggest that the DOX-induced aortic relaxation dysfunction is not caused by impaired levels of αSMA. OPN is crucial when the cardiovascular system has been damaged. This compound in the extracellular matrix is essential for scar formation and healing. However, when there is a dysregulation of OPN functioning during, for example, disease or damage, fibrosis can develop (70). However, we observed no difference in OPN content between groups. We can conclude that there is no increase in OPN activity in aortae when animals were treated with DOX chemotherapy compared to CTRL animals. Consequently, other components then αSMA or OPN, such as NO signaling or eNOS, an enzyme that produces NO, could be underlying the DOX-induced toxicity.

4.7 Challenges and prospects. In this research, we show that DOX causes significant acute and chronic damage to aortae and cardiomyocytes. In addition to this, we demonstrate the cardiovascular protective effects of SOD and PM.

SOD, known to be a superoxide scavenger and thus to reduce oxidative stress, was partly able to improve the DOX-induced damage to aortae *ex vivo*. This provides interesting new insights into the mechanisms by which DOX induces cardiovascular dysfunction. For follow-up studies, it would be ideal to measure oxidative stress based on, for example, based on the oxidation of 2′,7′-dichlorodihydrofluorescein to a fluorescent 2′,7′-dichlorofluorescein (Kalivendi *et al.* (46)). These data will indicate the levels of oxidative stress after DOX treatment and the effect of SOD on this. Additionally, PM (used in the *in vivo* study) can also be included to test its effect on oxidative stress levels after DOX treatment. Mitochondria have an important role in oxidative stress. Because these organelles are responsible for ATP production via the respiratory chain, they can be involved in the production of ROS via one-electron carriers (71). Consequently, performing a toluidine blue staining of mitochondria in cardiomyocytes and aorta's smooth muscle cells or evaluating ATP levels in these cells are ideal experiments to include in a next study. This will provide insights into the role of mitochondria in DOX-induced cardiovascular toxicity.

However, as suggested by this study, more mechanisms are involved in the DOX-induced cardiovascular toxicity. Soluble guanylate cyclase (sGC), such as vericiguat, could possibly be involved in the aortic dysfunction (72). Another mechanism that could be involved in DOX-induced aortic toxicity is NO production, a compound important for relaxation (73). For a follow-up study, evaluating NO levels after DOX treatment is an added value to investigate how DOX induces toxicity and as a therapeutical target. Basal NO levels can be determined by using Nω-nitro-l-arginine methyl ester (L- NAME), an eNOS blocker (Bosman *et al.* (23)). Based on the contraction after PE and after PE+L-NAME, basal NO levels can be determined. Data will provide insights into the influence of DOX on the NO levels. A combination of multiple compounds targeting the toxic consequences of DOX could possibly give a synergistic effect and might be interesting for future experiments. Using both solo and combinatorial treatments will provide better insights into the mechanisms by which DOX causes detrimental effects on the cardiovascular system. Additionally, assessing the effect of this treatment on cardiomyocytes will contribute to our knowledge of DOX-induced toxicity.

As previously mentioned, Ca^{2+} levels can be disrupted by DOX, consequently causing contractile dysfunction in cardiomyocytes. To assess Ca^{2+} levels, an in-house well-established method, known as whole-cell ruptured patch clamp (Deluyker *et al.* (33)), can be included in a next study. This technique provides insights into the Ca^{2+} current through the L-type channels and consequently the effect of DOX on the Ca^{2+} levels can be evaluated.

In this study, DOX-induced toxicity in cardiomyocytes after *in vivo* DOX-treatment was investigated. In future studies, vasomotor experiments of aortae of *in vivo* DOX-treated animals should also be included to assess relaxation and contraction. When, for example, an impaired contraction or relaxation is observed in aortae of DOX animals, these effects can be due to NO dysfunction (see above), since NO has been shown to be important in DOX-induced impaired relaxation (Bosman *et al. (23)*).

Our results and other literature suggest an important role in DOX-induced toxicity. This highlights the importance of further assessing the anti-inflammatory effects of PM in cardiac tissue. In a follow-up study, more inflammatory cells (e.g., T lymphocyte subset, $CD25^+$ regulatory T lymphocytes) should be investigated. Additionally, aortae can be included to assess inflammation in aortic tissue. When targeting PM specifically to the cardiovascular system (see below), the anti-inflammatory properties of PM could possibly improve the inflammation better.

In the *in vivo* study, a cumulative dose of 16 mg/kg was used. Currently, clinicians use a cumulative dose of 400-450 mg/m² (16 mg/kg) in human patients to limit severe DOX-induced cardiotoxicity, which is comparable to a dose of 16 mg/kg (4). In a follow-up study, this cumulative dose will be used again to ensure translatability. In this study, the DOX animal used is a non-tumor bearing model. In a follow-up study, a breast cancer rat model will be used to assess the cardioprotective effects of PM on DOX-treated tumor-bearing animals. This gives insights into the effect of PM on tumor and tumor progression and improves the translatability of this research to human patients. In addition to this, this follow-up study will provide new

insights into how PM could be implemented in the basic treatment strategies of cancer patients. Additionally, a longer-term study should be done. Cardiovascular function should be assessed during several intervals (e.g., months) after doxorubicin chemotherapy is done to investigate the detrimental effects later in life, as is also seen in human patients where serious cardiovascular problems arise after a chemotherapy session is finished.

Because PM is administered via drinking water, a substantial amount of PM can get lost. To overcome this, targeting PM specifically to the cardiovascular system can decrease loss of PM and increase specificity. PM could be injected i.p., since i.p. injections have better bioavailability and faster uptake compared to oral administration (74). PM could also be loaded in solid lipid nanoparticles (SLN) to improve bioavailability and to specifically reach the target organs. Additionally, because PM can be released at a constant, controlled rate, one injection during a certain period (e.g., every eight weeks) would be sufficient. These PM-containing SLN particles can be administered via a parental injection (e.g., intramuscular) to further improve bioavailability (75, 76). When PM shows to be beneficial in a tumor-bearing animal model, PM can be tested in clinical settings. Since administering PM in drinking water to patients would be inconvenient (e.g., monitoring, other drinks), the mode of administrating PM is another important advantage. The PM-containing SLN particles might provide a good way of administering PM to cancer patients.

To conclude, additional research is highly necessary to investigate the mechanisms by which DOX causes cardiovascular toxicity. Based on these findings, therapeutical targets can be defined to provide the most optimal cardioprotective treatment for cancer patients during doxorubicin chemotherapy. PM and SOD are potential therapeutics to target these mechanisms (Figure 9).

5 CONCLUSION

We show that PM has significant cardioprotective effects. Relaxation was not impaired after chronic treatment, demonstrating that DOX mainly affects contractile properties. PM was able to improve the increase in TTP of cardiomyocytes after chronic DOX treatment *in vivo*. Additionally, we demonstrate the role of

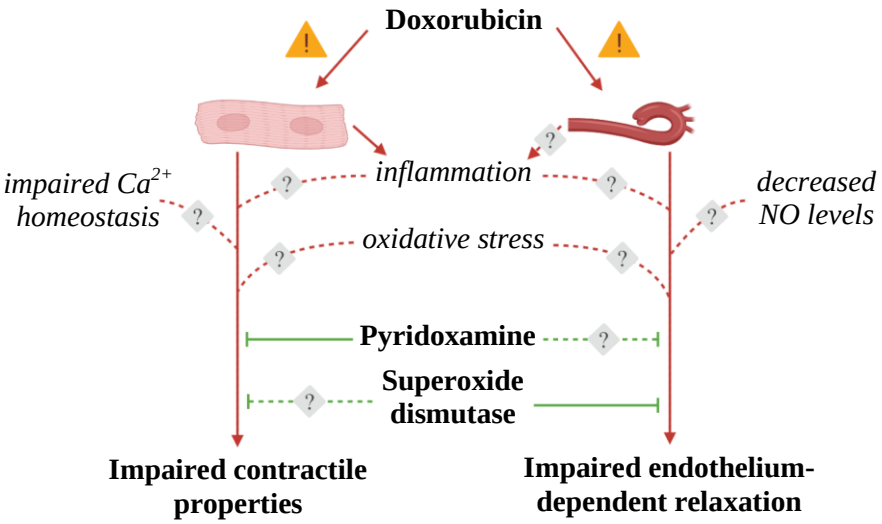

Figure 9. Potential mechanisms by which DOX causes cardiovascular toxicity. We show that chronic DOX exposure induces impaired contractile properties in cardiomyocytes and that acute DOX incubation causes impaired endothelium-dependent relaxation in aortae. Based on our findings and on literature, impaired Ca^{2+} homeostasis, decreased NO levels, and inflammation might underly these toxicities. However, additional research is needed to define the exact mechanisms to provide therapeutical targets. We demonstrate the cardiovascular protective properties of PM and SOD. *DOX, doxorubicin; NO, nitric oxide; PM, pyridoxamine; SOD, superoxide dismutase.*

oxidative stress in DOX-induced aortic damage. SOD could partially improve impaired endothelium-dependent aortic relaxation after acute DOX incubation, suggesting that DOX causes toxicity via multiple mechanisms. Taken together all the findings, DOX causes its toxicity via several different mechanisms. This highlights the importance of more research into DOX-induced toxicity to find the most potent, beneficial cardioprotective compound. In the long term, PM can possibly be included in the general cancer treatment to diminish or prevent cardiotoxicity and aortic damage in cancer patients. PM can be able to decrease cardiovascular problems in cancer patients. In addition to this, we also demonstrate that oxidative stress is a mechanism used by DOX, causing toxicity to aortic function.

6 REFERENCES

1. Franco YL, Vaidya TR, Ait-Oudhia S. Anticancer and cardio-protective effects of liposomal doxorubicin in the treatment of breast cancer. Breast Cancer (Dove Med Press). 2018;10:131-41.
2. Pollack SM, Redman MW, Baker KK, Wagner MJ, Schroeder BA, Loggers ET, et al. Assessment of Doxorubicin and Pembrolizumab in Patients With Advanced Anthracycline-Naive Sarcoma: A Phase 1/2 Nonrandomized Clinical Trial. JAMA Oncol. 2020;6(11):1778-82.
3. Renu K, Abilash V, PB TP, Arunachalam S. Molecular mechanism of doxorubicin-induced cardiomyopathy–An update. European journal of pharmacology. 2018;818:241-53.
4. Quintana RA, Banchs J, Gupta R, Lin HY, Raj SD, Conley A, et al. Early evidence of cardiotoxicity and tumor response in patients with sarcomas after high cumulative dose doxorubicin given as a continuous infusion. Sarcoma. 2017;2017.
5. Cho H, Lee S, Sim SH, Park IH, Lee KS, Kwak MH, et al. Cumulative incidence of chemotherapy-induced cardiotoxicity during a 2-year follow-up period in breast cancer patients. Breast cancer research and treatment. 2020;182:333-43.
6. Shi Y, Moon M, Dawood S, McManus B, Liu P. Mechanisms and management of doxorubicin cardiotoxicity. Herz. 2011;36(4):296-305.
7. Madabhushi R. The Roles of DNA Topoisomerase IIbeta in Transcription. Int J Mol Sci. 2018;19(7).
8. McGowan JV, Chung R, Maulik A, Piotrowska I, Walker JM, Yellon DM. Anthracycline chemotherapy and cardiotoxicity. Cardiovascular drugs and therapy. 2017;31(1):63-75.
9. Reichardt P, Tabone M-D, Mora J, Morland B, Jones RL. Risk–benefit of dexrazoxane for preventing anthracycline-related cardiotoxicity: re-evaluating the European labeling. Future oncology. 2018;14(25):2663-76.
10. Zhang S, Liu X, Bawa-Khalfe T, Lu L-S, Lyu YL, Liu LF, et al. Identification of the molecular basis of doxorubicin-induced cardiotoxicity. Nature medicine. 2012;18(11):1639-42.
11. Singal PK, Iliskovic N. Doxorubicin-induced cardiomyopathy. New England Journal of Medicine. 1998;339(13):900-5.
12. Patnaik JL, Byers T, DiGuiseppi C, Dabelea D, Denberg TD. Cardiovascular disease competes with breast cancer as the leading cause of death for older females diagnosed with breast cancer: a retrospective cohort study. Breast Cancer Research. 2011;13(3):1-9.
13. Bradshaw PT, Stevens J, Khankari N, Teitelbaum SL, Neugut AI, Gammon MD. Cardiovascular disease mortality among breast cancer survivors. Epidemiology (Cambridge, Mass). 2016;27(1):6.
14. Yeh ET, Tong AT, Lenihan DJ, Yusuf SW, Swafford J, Champion C, et al. Cardiovascular complications of cancer therapy: diagnosis, pathogenesis, and management. Circulation. 2004;109(25):3122-31.
15. Wang Y, Branicky R, Noe A, Hekimi S. Superoxide dismutases: Dual roles in controlling ROS damage and regulating ROS signaling. J Cell Biol. 2018;217(6):1915-28.
16. Carvalho FS, Burgeiro A, Garcia R, Moreno AJ, Carvalho RA, Oliveira PJ. Doxorubicin-induced cardiotoxicity: from bioenergetic failure and cell death to cardiomyopathy. Medicinal research reviews. 2014;34(1):106-35.

17. Chatterjee K, Zhang J, Honbo N, Karliner JS. Doxorubicin cardiomyopathy. Cardiology. 2010;115(2):155-62.
18. Lipshultz SE, Colan SD, Gelber RD, Perez-Atayde AR, Sallan SE, Sanders SP. Late cardiac effects of doxorubicin therapy for acute lymphoblastic leukemia in childhood. N Engl J Med. 1991;324(12):808-15.
19. Gibson NM, Greufe SE, Hydock DS, Hayward R. Doxorubicin-induced vascular dysfunction and its attenuation by exercise preconditioning. J Cardiovasc Pharmacol. 2013;62(4):355-60.
20. Olukman M, Can C, Erol A, Oktem G, Oral O, Cinar MG. Reversal of doxorubicin-induced vascular dysfunction by resveratrol in rat thoracic aorta: Is there a possible role of nitric oxide synthase inhibition? Anadolu Kardiyol Derg. 2009;9(4):260-6.
21. Wojcik T, Buczek E, Majzner K, Kolodziejczyk A, Miszczyk J, Kaczara P, et al. Comparative endothelial profiling of doxorubicin and daunorubicin in cultured endothelial cells. Toxicology In Vitro. 2015;29(3):512-21.
22. Murata T, Yamawaki H, Yoshimoto R, Hori M, Sato K, Ozaki H, et al. Chronic effect of doxorubicin on vascular endothelium assessed by organ culture study. Life sciences. 2001;69(22):2685-95.
23. Bosman M, Favere K, Neutel CHG, Jacobs G, De Meyer GRY, Martinet W, et al. Doxorubicin induces arterial stiffness: A comprehensive in vivo and ex vivo evaluation of vascular toxicity in mice. Toxicol Lett. 2021;346:23-33.
24. Hodjat M, Haller H, Dumler I, Kiyan Y. Urokinase receptor mediates doxorubicin-induced vascular smooth muscle cell senescence via proteasomal degradation of TRF2. J Vasc Res. 2013;50(2):109-23.
25. Budinskaya K, Puchnerova V, Svacinova J, Novak J, Hrstkova H, Novakova M, et al. Non-invasive assessment of vascular system function and damage induced by anthracycline treatment in the pediatric cancer survivors. Physiol Res. 2017;66(Suppl 4):S553-S60.
26. Chaosuwannakit N, D'Agostino Jr R, Hamilton CA, Lane KS, Ntim WO, Lawrence J, et al. Aortic stiffness increases upon receipt of anthracycline chemotherapy. Journal of clinical oncology. 2010;28(1):166.
27. Perrone A, Giovino A, Benny J, Martinelli F. Advanced glycation end products (AGEs): biochemistry, signaling, analytical methods, and epigenetic effects. Oxidative medicine and cellular longevity. 2020;2020.
28. Rasool M, Malik A, Butt TT, Ashraf MAB, Rasool R, Zahid A, et al. Implications of advanced oxidation protein products (AOPPs), advanced glycation end products (AGEs) and other biomarkers in the development of cardiovascular diseases. Saudi journal of biological sciences. 2019;26(2):334-9.
29. Hegab Z, Gibbons S, Neyses L, Mamas MA. Role of advanced glycation end products in cardiovascular disease. World journal of cardiology. 2012;4(4):90.
30. Haesen S, Cöl Ü, Schurgers W, Evens L, Verboven M, Driesen RB, et al. Glycolaldehyde-modified proteins cause adverse functional and structural aortic remodeling leading to cardiac pressure overload. Scientific reports. 2020;10(1):1-14.
31. Del Turco S, Navarra T, Gastaldelli A, Basta G. Protective role of adiponectin on endothelial dysfunction induced by AGEs: a clinical and experimental approach. Microvascular research. 2011;82(1):73-6.
32. Ren X, Ren L, Wei Q, Shao H, Chen L, Liu N. Advanced glycation end-products decreases expression of endothelial nitric oxide synthase through oxidative stress in human coronary artery endothelial cells. Cardiovascular diabetology. 2017;16(1):1-12.
33. Deluyker D, Evens L, Haesen S, Driesen RB, Kuster D, Verboven M, et al. Glycolaldehyde-derived high-molecular-weight advanced glycation end-products induce cardiac dysfunction through structural and functional remodeling of cardiomyocytes. Cellular physiology and biochemistry: international journal of experimental cellular physiology, biochemistry, and pharmacology. 2020;54(5):809-24.
34. Deluyker D, Ferferieva V, Driesen RB, Verboven M, Lambrichts I, Bito V. Pyridoxamine improves survival and limits cardiac dysfunction after MI. Scientific reports. 2017;7(1):1-12.
35. Ramis R, Ortega-Castro J, Caballero C, Casasnovas R, Cerrillo A, Vilanova B, et al. How does pyridoxamine inhibit the formation of advanced glycation end products? The role of its primary antioxidant activity. Antioxidants. 2019;8(9):344.

36. Zhang X, Xu L, Chen W, Yu X, Shen L, Huang Y. Pyridoxamine alleviates mechanical allodynia by suppressing the spinal receptor for advanced glycation end product-nuclear factor-κ B/extracellular signal-regulated kinase signaling pathway in diabetic rats. Molecular pain. 2020;16:1744806920917251.
37. Voziyan P, Hudson B. Pyridoxamine as a multifunctional pharmaceutical: targeting pathogenic glycation and oxidative damage. Cellular and Molecular Life Sciences CMLS. 2005;62(15):1671-81.
38. Carrasco R, Castillo RL, Gormaz JG, Carrillo M, Thavendiranathan P. Role of oxidative stress in the mechanisms of anthracycline-induced cardiotoxicity: effects of preventive strategies. Oxidative medicine and cellular longevity. 2021;2021.
39. Xu H, Yu W, Sun S, Li C, Zhang Y, Ren J. Luteolin attenuates doxorubicin-induced cardiotoxicity through promoting mitochondrial autophagy. Frontiers in physiology. 2020;11:113.
40. Gorini S, De Angelis A, Berrino L, Malara N, Rosano G, Ferraro E. Chemotherapeutic drugs and mitochondrial dysfunction: focus on doxorubicin, trastuzumab, and sunitinib. Oxidative medicine and cellular longevity. 2018;2018.
41. Rawat PS, Jaiswal A, Khurana A, Bhatti JS, Navik U. Doxorubicin-induced cardiotoxicity: An update on the molecular mechanism and novel therapeutic strategies for effective management. Biomed Pharmacother. 2021;139:111708.
42. Gonzalez-Hunt CP, Wadhwa M, Sanders LH. DNA damage by oxidative stress: Measurement strategies for two genomes. Current Opinion in Toxicology. 2018;7:87-94.
43. Dewenter M, von der Lieth A, Katus HA, Backs J. Calcium signaling and transcriptional regulation in cardiomyocytes. Circulation research. 2017;121(8):1000-20.
44. Bosman M, Krüger DN, Favere K, Wesley CD, Neutel CH, Van Asbroeck B, et al. Doxorubicin Impairs Smooth Muscle Cell Contraction: Novel Insights in Vascular Toxicity. International Journal of Molecular Sciences. 2021;22(23):12812.
45. Keyer K, Imlay JA. Superoxide accelerates DNA damage by elevating free-iron levels. Proceedings of the National Academy of Sciences. 1996;93(24):13635-40.
46. Kalivendi SV, Kotamraju S, Zhao H, Joseph J, Kalyanaraman B. Doxorubicin-induced apoptosis is associated with increased transcription of endothelial nitric-oxide synthase: effect of antiapoptotic antioxidants and calcium. Journal of Biological Chemistry. 2001;276(50):47266-76.
47. Kotamraju S, Konorev EA, Joseph J, Kalyanaraman B. Doxorubicin-induced apoptosis in endothelial cells and cardiomyocytes is ameliorated by nitrone spin traps and ebselen: role of reactive oxygen and nitrogen species. Journal of Biological Chemistry. 2000;275(43):33585-92.
48. Hattori Y, Kawasaki H, Abe K, Kanno M. Superoxide dismutase recovers altered endothelium-dependent relaxation in diabetic rat aorta. American Journal of Physiology-Heart and Circulatory Physiology. 1991;261(4):H1086-H94.
49. Lund DD, Gunnett CA, Chu Y, Brooks RM, Faraci FM, Heistad DD. Gene transfer of extracellular superoxide dismutase improves relaxation of aorta after treatment with endotoxin. American Journal of Physiology-Heart and Circulatory Physiology. 2004;287(2):H805-H11.
50. Li X, Gu J, Zhang Y, Feng S, Huang X, Jiang Y, et al. L-arginine alleviates doxorubicin-induced endothelium-dependent dysfunction by promoting nitric oxide generation and inhibiting apoptosis. Toxicology. 2019;423:105-11.
51. Kim J-E, Choi B-K, Choi J-Y, Ryu T, Roh WS, Song S-Y. Role of calcium channels responsible for phenylephrine-induced contraction in rat aorta 3 days after acute myocardial infarction. Korean Journal of Anesthesiology. 2014;66(2):143.
52. Zhang X, Hu C, Kong C-Y, Song P, Wu H-M, Xu S-C, et al. FNDC5 alleviates oxidative stress and cardiomyocyte apoptosis in doxorubicin-induced cardiotoxicity via activating AKT. Cell Death & Differentiation. 2020;27(2):540-55.
53. Takaseya T, Ishimatsu M, Tayama E, Nishi A, Akasu T, Aoyagi S. Mechanical unloading improves intracellular Ca2+ regulation in rats with doxorubicin-induced cardiomyopathy. Journal of the American College of Cardiology. 2004;44(11):2239-46.
54. Hu X, Liu H, Wang Z, Hu Z, Li L. miR-200a attenuated doxorubicin-induced cardiotoxicity through upregulation of Nrf2 in mice. Oxidative medicine and cellular longevity. 2019;2019.
55. Wang J, Li P, Xu X, Zhang B, Zhang J. MicroRNA-200a inhibits inflammation and atherosclerotic lesion formation by disrupting EZH2-mediated methylation of STAT3. Frontiers in Immunology. 2020;11:907.

56. Ma Y, Pan C, Tang X, Zhang M, Shi H, Wang T, et al. MicroRNA-200a represses myocardial infarction-related cell death and inflammation by targeting the Keap1/Nrf2 and β-catenin pathways. Hellenic Journal of Cardiology. 2021;62(2):139-48.
57. Klinge U, Dievernich A, Tolba R, Klosterhalfen B, Davies L. CD68+ macrophages as crucial components of the foreign body reaction demonstrate an unconventional pattern of functional markers quantified by analysis with double fluorescence staining. Journal of Biomedical Materials Research Part B: Applied Biomaterials. 2020;108(8):3134-46.
58. Zhang H, Xu A, Sun X, Yang Y, Zhang L, Bai H, et al. Self-maintenance of cardiac resident reparative macrophages attenuates doxorubicin-induced cardiomyopathy through the SR-A1-C-MYC axis. Circulation Research. 2020;127(5):610-27.
59. Xinyong C, Zhiyi Z, Lang H, Peng Y, Xiaocheng W, Ping Z, et al. The role of toll-like receptors in myocardial toxicity induced by doxorubicin. Immunology letters. 2020;217:56-64.
60. Katare PB, Bagul PK, Dinda AK, Banerjee SK. Toll-like receptor 4 inhibition improves oxidative stress and mitochondrial health in isoproterenol-induced cardiac hypertrophy in rats. Frontiers in Immunology. 2017;8:719.
61. Fang W, Bi D, Zheng R, Cai N, Xu H, Zhou R, et al. Identification and activation of TLR4-mediated signalling pathways by alginate-derived guluronate oligosaccharide in RAW264. 7 macrophages. Scientific reports. 2017;7(1):1-13.
62. Yu L, Feng Z. The role of toll-like receptor signaling in the progression of heart failure. Mediators of inflammation. 2018;2018.
63. Wang L, Chen Q, Qi H, Wang C, Wang C, Zhang J, et al. Doxorubicin-induced systemic inflammation is driven by upregulation of toll-like receptor TLR4 and endotoxin leakage. Cancer research. 2016;76(22):6631-42.
64. Zhang J, Herman EH, Ferrans V. Dendritic cells in the hearts of spontaneously hypertensive rats treated with doxorubicin with or without ICRF-187. The American journal of pathology. 1993;142(6):1916.
65. Alyamkina EA, Nikolin VP, Popova NA, Dolgova EV, Proskurina AS, Orishchenko KE, et al. A strategy of tumor treatment in mice with doxorubicin-cyclophosphamide combination based on dendritic cell activation by human double-stranded DNA preparation. Genetic vaccines and therapy. 2010;8(1):1-10.
66. Moriyama T, Kemi M, Okumura C, Yoshihara K, Horie T. Involvement of advanced glycation end-products, pentosidine and Nε-(carboxymethyl) lysine, in doxorubicin-induced cardiomyopathy in rats. Toxicology. 2010;268(1-2):89-97.
67. Wang J, Zohar R, McCulloch CA. Multiple roles of α-smooth muscle actin in mechanotransduction. Experimental cell research. 2006;312(3):205-14.
68. Yuan S-M. α-Smooth muscle actin and ACTA2 gene expressions in vasculopathies. Brazilian journal of cardiovascular surgery. 2015;30:644-9.
69. Guo D-C, Pannu H, Tran-Fadulu V, Papke CL, Yu RK, Avidan N, et al. Mutations in smooth muscle α-actin (ACTA2) lead to thoracic aortic aneurysms and dissections. Nature genetics. 2007;39(12):1488-93.
70. Abdelaziz Mohamed I, Gadeau A-P, Hasan A, Abdulrahman N, Mraiche F. Osteopontin: a promising therapeutic target in cardiac fibrosis. Cells. 2019;8(12):1558.
71. Lenaz G. Role of mitochondria in oxidative stress and ageing. Biochimica et Biophysica Acta (BBA)-Bioenergetics. 1998;1366(1-2):53-67.
72. Information NCfB. PubChem Compound Summary for CID 54674461, Vericiguat 2022 [Available from: https://pubchem.ncbi.nlm.nih.gov/compound/Vericiguat.
73. Gantner BN, LaFond KM, Bonini MG. Nitric oxide in cellular adaptation and disease. Redox Biology. 2020;34:101550.
74. Techniques in the Behavioral and Neural Sciences1994.
75. Iqbal MA, Md S, Sahni JK, Baboota S, Dang S, Ali J. Nanostructured lipid carriers system: recent advances in drug delivery. J Drug Target. 2012;20(10):813-30.
76. Üner M, Yener G. Importance of solid lipid nanoparticles (SLN) in various administration routes and future perspectives. International journal of nanomedicine. 2007;2(3):289.

Acknowledgements – First, I want to thank Sibren Haesen (*Ph.D. student, BIOMED, Diepenbeek, Belgium*), my daily supervisor who supported my research on a daily basis. I am very grateful for his guidance through the project and for allowing me to improve my practical and critical thinking skills. Also, I appreciate he took the time to provide feedback on my process during the internship and to review my thesis. I am extremely thankful for all the tips and skills he taught me during my internship period. Because of his guidance, I feel I am a better scientist, both inside and outside the lab. Sibren was always there when I had a question or problem. This was a nice feeling and I felt appreciated. I also want to thank Sibren for the opportunity to take over the fwo Instagram for one week together. I liked communicating our research to the Instagram followers and feeling like an 'instagrammer' for one week (;-)).

I would like to express my appreciation to dr. Dorien Deluyker *(Doctor-assistant, BIOMED, Diepenbeek, Belgium*). She also supported me a lot during my internship, and she provided very helpful tips and tricks for performing research. She was always there when I had a question for her; she really has a heart of gold. I would like to thank Dorien for her time to review my thesis and for providing feedback.

I would like to gratefully thank my principal supervisor, Prof. Virginio Bito, for giving me the opportunity of doing my internship in her research group, in spite of me not having a lot of experience in the field of cardiology. I enjoyed being part of her research group and I felt really welcome to the team. Prof. Bito showed interest in my research, I really felt appreciated. Because of her work in DR Congo, I got stimulated to not only focus on our current research but also look further than our own research facility. Thank you for this!

In addition to this, I am very grateful to the whole team of the Department of cardio- and organs systems of the University of Hasselt. I want to thank them for their help during the project. I would like to thank Prof. dr. Esther Wolfs, Sarah D'Haese, and Ellen Heeren. They are thanked for their help during experiments and for their help during the research in general.

Lastly, I am very grateful to my closest family: my mom and sister. I appreciate their unlimited support a lot and I really felt supported during my internship. Thank you!

I wish you all the very best in performing research, in finishing Ph.D. theses, and in life in general! Thank you!

Author contributions – V.B., E.W., D.D., and S.H set up the experimental design. D.D., S.H., and M.M.J. executed experiments and analyzed data. This manuscript was written by M.M.J. The work was critically reviewed by D.D. and S.H.

SUPPLEMENTARY

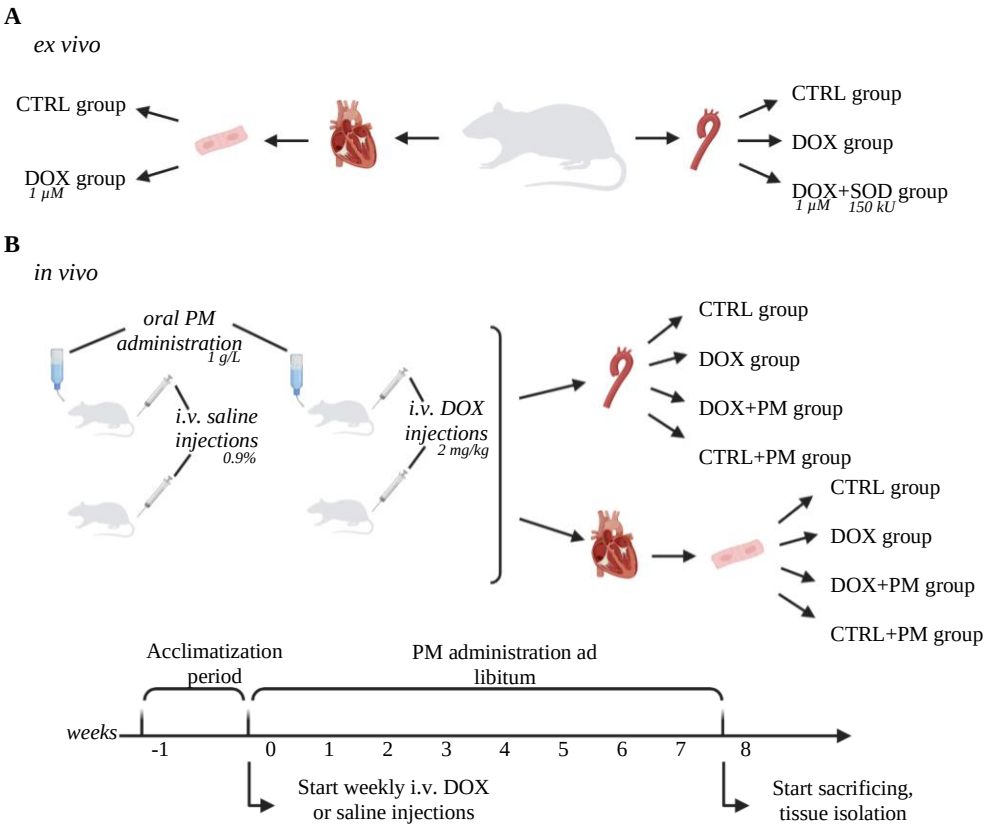

Supplementary Figure 1. Experimental design. **A.** Heart and aorta were isolated immediately after sacrificing. Cardiomyocytes were isolated from the heart and divided into two groups: CTRL and DOX (2 h incubation). Aortae were divided into three groups: CTRL, DOX (2 h incubation), and DOX+SOD (2 h incubation). Aortae were assessed on vasomotor function and cardiomyocytes on contractile response. **B.** After one week of acclimatization, treatments started for eight weeks. DOX (2 mg/kg) or saline (0.9%) were i.v. administered on a weekly basis. PM was given ad libitum in the drinking water. Isolation of the tissues and experiments started eight weeks after the start of treatments. *PM, pyridoxamine; DOX, doxorubicin.*

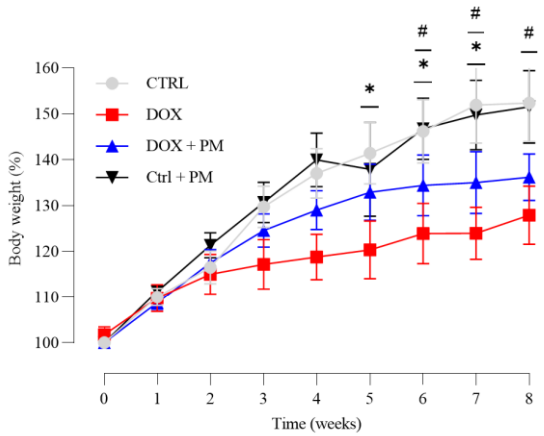

Supplementary Figure 2. DOX-treated animals show a significantly lower body weight compared to CTRL animals. DOX (2 mg/kg) was injected weekly for eight weeks. PM was given ad libitum. Body weight of CTRL ($N_{animals}$=7), DOX ($N_{animals}$=8), DOX+PM ($N_{animals}$=9), and CTRL+PM ($N_{animals}$=7) group. Data are shown as mean ± SEM. *DOX, doxorubicin; PM, pyridoxamine.* *p<0.05, DOX vs CTRL; #p<0.05, DOX+PM vs CTRL

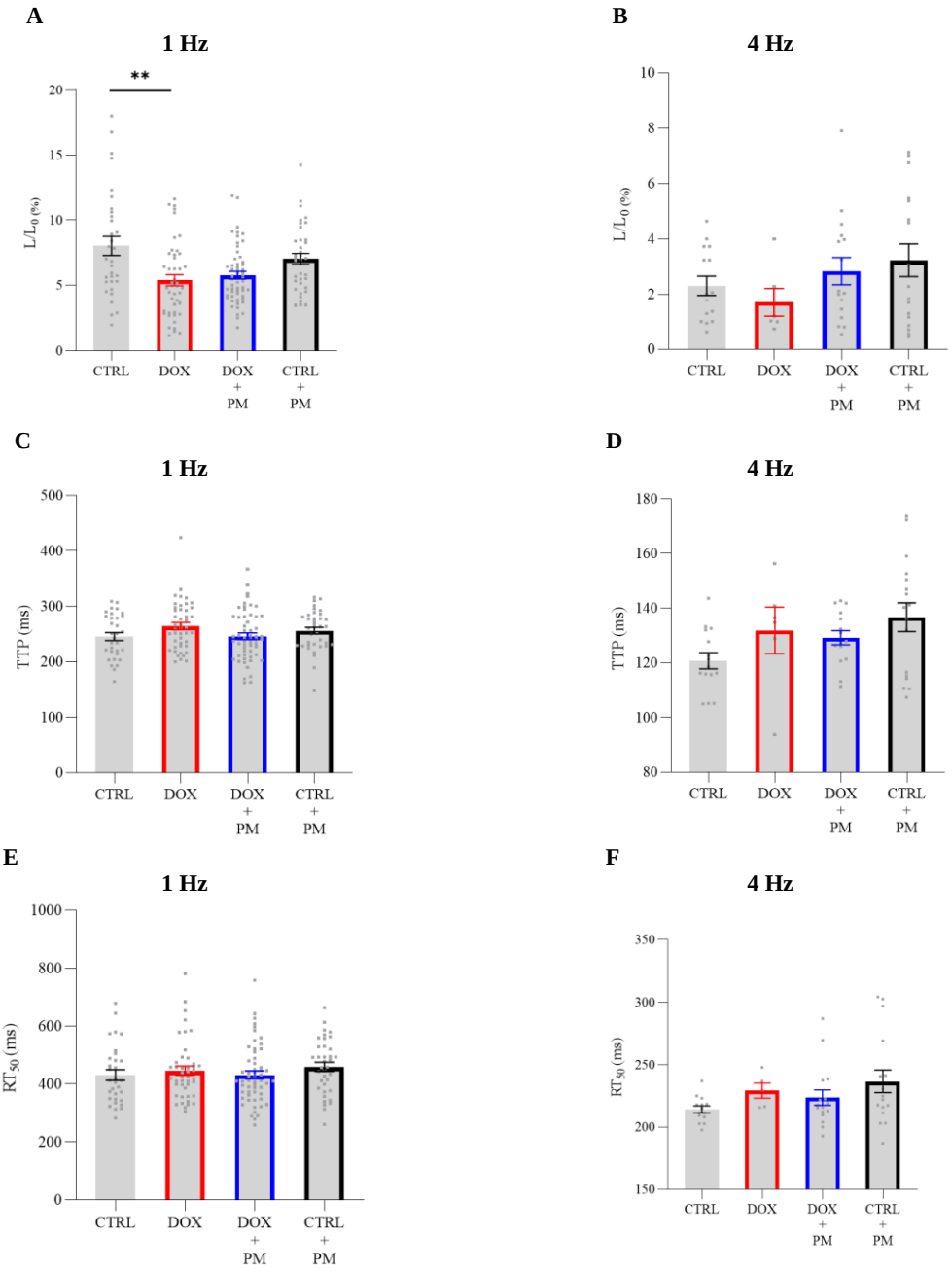

Supplementary Figure 3. DOX causes significant impairment in contractile response of cardiomyocytes *in vivo* at 1 Hz. DOX treated animals received weekly i.v. DOX injections (2 mg/kg) for eight weeks. PM treated animals received PM ad libitum via drinking water. CTRL animals were left untreated. Cardiomyocytes were isolated from the heart via enzymatic dissociation and cell measurements were performed at 1 Hz ($N_{animals}$CTRL=5, $N_{animals}$DOX=7, $N_{animals}$DOX+PM=8, $N_{animals}$CTRL+PM=7) and 4 Hz ($N_{animals}$CTRL=5, $N_{animals}$DOX=4, $N_{animals}$DOX+PM=7, $N_{animals}$CTRL+PM=5). **A.** Fractional cell shortening at 1 Hz (n_{cells}CTRL=32, n_{cells}DOX=45, n_{cells}DOX+PM=55, n_{cells}CTRL+PM=37). **B.** Fractional cell shortening at 4 Hz (n_{cells}CTRL=15, n_{cells}DOX=6, n_{cells}DOX+PM=16, n_{cells}CTRL+PM=17). **C.** Time to peak at 1 Hz (n_{cells}CTRL=32, n_{cells}DOX=45, n_{cells}DOX+PM=56, n_{cells}CTRL+PM=37). **D.** Time to peak at 4 Hz (n_{cells}CTRL=15, n_{cells}DOX=6, n_{cells}DOX+PM=15, n_{cells}CTRL+PM=17). **E.** Time to 50% relaxation at 1 Hz (n_{cells}CTRL=31, n_{cells}DOX=44, n_{cells}DOX+PM=56, n_{cells}CTRL+PM=37). **F.** Time to 50% relaxation at 4 Hz (n_{cells}CTRL=14, n_{cells}DOX=5, n_{cells}DOX+PM=16, n_{cells}CTRL+PM=16). Data are shown as mean ± SEM. *DOX, doxorubicin; PM, pyridoxamine; L/L_0, fractional cell shortening normalized to cell length; TTP, time to peak; RT50, time to 50% relaxation.* **p<0.01

Supplementary Table 1 – Overview of cardiomyocyte responsiveness to 1 Hz, 2 Hz, and 4 Hz stimulation per animal.

	CTRL ($N_{animals}$=5)	**DOX** ($N_{animals}$=7)	**DOX+PM** ($N_{animals}$=8)	**CTRL+PM** ($N_{animals}$=7)
1 Hz	100	100	100	100
2 Hz	100	84 ± 7	78 ± 11	91 ± 4
4 Hz	43 ± 6	21 ± 10	26 ± 8	38 ± 14

Cardiomyocytes per group that responded to 2 Hz and 4 Hz stimulation compared to 1 Hz stimulation per group, shown in percentages. Data are shown as mean ± SEM. *DOX, doxorubicin; PM, pyridoxamine; N, number of animals of which cardiomyocytes were isolated.*

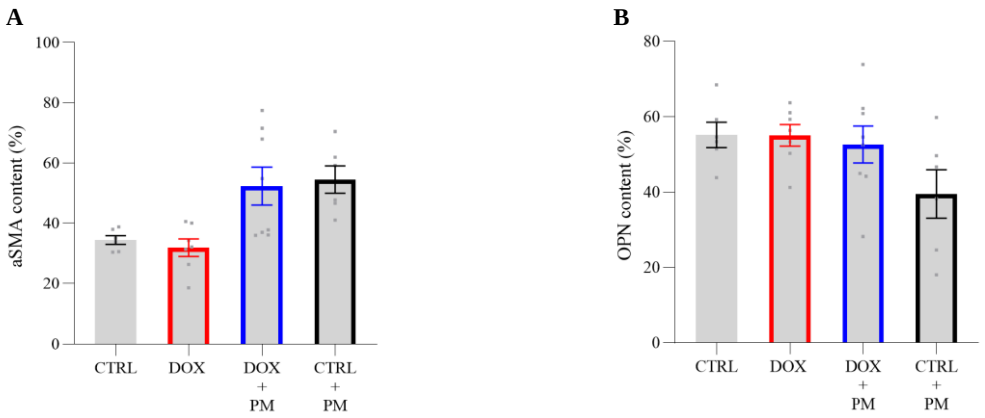

Supplementary Figure 4. No differences were found in αSMA or OPN content in aortae after DOX treatment. Animals were divided into four groups: CTRL, DOX, DOX+PM, and CTRL+PM. After eight weeks of weekly DOX treatment (2 mg/kg) and PM administration at libitum, aortae were isolated and IHC was performed. For every animal, on average eight random fields were used to assess staining. **A.** αSMA ($N_{animals}$ CTRL=6; $N_{animals}$DOX=7, $N_{animals}$DOX+PM=8, $N_{animals}$CTRL+PM=6)). **B.** OPN ($N_{animals}$CTRL=6, $N_{animals}$DOX=7, $N_{animals}$DOX+PM=8, $N_{animals}$CTRL+PM=6). Images were analyzed with ImageJ. Data are shown as mean ± SEM. *αSMA, smooth muscle alpha-actin; OPN, osteopontin; DOX, doxorubicin; PM, pyridoxamine; IHC, immunohistochemistry.*